PNAS
www.pnas.org

SUPPLEMENTARY INFORMATION FOR

The generality of cryptic dietary niche differences in diverse large-herbivore assemblages

Johan Pansu, Matthew C. Hutchinson, T. Michael Anderson, Mariska te Beest, Colleen Begg, Keith Begg, Aurelie Bonin, Lackson Chama, Simon Chamaillé-Jammes, Eric Coissac, Joris P.G.M. Cromsigt, Margaret Y. Demmel, Jason E. Donaldson, Jennifer A. Guyton, Christina B. Hansen, Christopher I. Imakando, Azwad Iqbal, Davis F. Kalima, Graham I.H. Kerley, Samson Kurukura, Marietjie Landman, Ryan A. Long, Isaack Norbert Munuo, Ciara M. Nutter, Catherine L. Parr, Arjun B. Potter, Stanford Siachoono, Pierre Taberlet, Eusebio Waiti, Tyler R. Kartzinel, Robert M. Pringle

Corresponding authors: Johan Pansu and Robert M. Pringle
Emails: johan.pansu@gmail.com, rpringle@princeton.edu

This PDF file includes:

Other supplementary materials for this manuscript include the following:

Datasets S1–S25

TEXT S1. SUPPLEMENTARY MATERIALS AND METHODS

Herbivore taxonomy and traits

We grouped herbivore species by widely accepted Latin binomials, ignoring subspecific designations. The taxonomy of dik-dik in Laikipia (central Kenya) is uncertain; *Madoqua guentheri* and *M. cavendishi* have been used previous studies. We use *Madoqua* cf. *guentheri*. The generic epithet for eland is variously given as *Tragelaphus* or *Taurotragus*; we used the former in light of molecular evidence that *Tragelaphus* is paraphyletic with respect to *Taurotragus* (1). We classified species as either ruminants (bovids and giraffe) or nonruminants; hippopotamus, a foregut-fermenting but nonruminating 'pseudoruminant', was included in the latter group. Herbivore body sizes are from PanTHERIA (2). Several domesticated ungulates co-occur with wildlife at our Laikipia site (3), but we excluded them from this study because their foraging is influenced by human herders.

Sample collection and DNA extraction

Salient attributes of our 10 study sites are summarized in **Table S1**. Methods for samples collected in Laikipia, Serengeti (Tanzania), Niassa (Mozambique), Gorongosa (Mozambique), Nyika (Malawi), Kafue (Zambia), Hwange (Zimbabwe), Hluhluwe-iMfolozi (South Africa) and Kruger (South Africa) are described in detail here. Although there were subtle differences in the pipeline used for some sets of these samples (described below), all samples were collected and processed in a similar way. Samples from Addo Elephant National Park (South Africa) were collected as part of an independent project; as a result, there were more substantive methodological differences in the way those samples were processed, which precluded certain comparative analyses (see *Addo samples*, below).

Fecal samples were collected and processed as described by Kartzinel et al. (4) and Pansu et al. (5). Fresh samples without any adhering plant tissue were collected in unused plastic bags and kept cool until returned to camp the same day, where they were pre-processed as follows. We homogenized samples by kneading the bag and then transferred ~200 mm^3 of sample (avoiding plant macroremains) into tubes containing silica beads and a stabilization/lysis buffer (Zymo Xpedition Stabilization/Lysis Solution, Zymo Research); tubes were vortexed for 30 s to lyse cells and then frozen for transport to Princeton University. Before import into the United States, samples were subjected to one of two antiviral treatments, as mandated by the US Department of Agriculture's Animal and Plant Health Inspection Service (permits 122489, 123156, 130123 to R.M.P.). Samples collected in Laikipia from 2013–2016 were treated with proteinase K, heated to 95°C for 15 min, and treated with RNase A. Following issuance of revised regulations, samples collected from 2016–2018 were subjected to heat-only treatment of 72°C for 30 min. On arrival at Princeton University, samples were frozen and stored at −80°C and later extracted in a facility dedicated to fecal DNA analysis, using Zymo Xpedition Soil/Fecal DNA MiniPrep kit according to manufacturer's instructions. We performed one extraction control (sample-free extract) per extraction batch (~20 to 30 samples).

PCR amplification and sequencing

We amplified a short and variable region of the chloroplast genome, the P6 loop of the *trn*L intron (4–6), using the universal primers

Forward (*g*): 5'-GGGCAATCCTGAGCCAA-3'
Reverse (*h*): 5'-CCATTGAGTCTCTGCACCTATC-3'

Tags composed of 8 base pairs (bp), each differing by ≥4 nucleotides, were added to the 5' end of each primer to enable the multiplexing of multiple PCR products per library before high-throughput sequencing (7, 8). PCRs were carried out in a 20 μL reaction volume including 2 μL template fecal DNA extract; 0.2 μM each primer; 0.2 mM each dNTP; 1X GenAmp PCR buffer II; 2.5 mM $MgCl_2$;

0.5U AmpliTaq Gold DNA Polymerase (Applied Biosystems); 4% dimethyl sulfoxide (Sigma-Aldrich); and 0.1 mg ml^{-1} of Bovine Serum Albumin (New England Biolabs). Thermocycling followed a program of initial denaturing at 95°C for 10 min, followed by 35 cycles of 95°C for 30 s, 55°C for 30 s, and 72°C for 30 s, with a 2-min final extension at 72°C. Extraction controls, PCR controls (using DNA-free water instead of DNA), and positive controls (made of DNA extract of known plants) were also amplified and later sequenced.

Amplification, purification, and sequencing strategies differed slightly between samples from Laikipia (2013–2016) and those collected in other sites (2016–2018). First, for all non-Laikipia samples, we performed multiple PCR replicates (2 or 3 per extract in 2016, 3 per extract in 2017 and 2018) to monitor reproducibility of results and stochasticity of the PCR and sequencing processes (9). Second, PCR products from Laikipia were purified using a SequalPrep Normalization Plate Kit (Applied Biosystems); for other sites, samples were pooled per plate and purified with a MinElute PCR Purification Kit (Qiagen). Finally, libraries for Laikipia samples were prepared using a PCR-based approach and sequenced in single-end (170 bp), whereas we used PCR-free library preparation and 2×150 bp paired-end sequencing for other sites. Samples from Laikipia in 2013 and 2016, Gorongosa in 2016, and Serengeti in 2017 and 2018 were all sequenced on separate sequencing runs. Samples from Laikipia in 2014 and 2015 were sequenced together, as were the 2017 samples from all sites except Serengeti; in these cases, samples from different sites/years were placed in different libraries. All libraries were sequenced on Illumina HiSeq 2500 platform at Princeton's Lewis-Sigler Institute for Integrative Genomics.

Data processing

Sequence data were curated using *OBITools* v.1.2 (10). For libraries sequenced in paired-end (i.e., all but those from Laikipia), paired-end reads were first aligned and assembled using the *Illuminapairedend* command; sequences with a low alignment-quality score (<40, the value corresponding to perfect alignment between the last 10 bases of each read) were discarded. Consensus sequences were then assigned to their original sample from the tag information attached to the primers, using the *ngsfilter* command (with default parameters allowing zero errors on tags and a maximum of two errors on primers). Identical sequences were merged with the *obiuniq* command, which retains information about their occurrence in each sample. Low-quality sequences were filtered out with *obigrep*; these included sequences with ambiguous nucleotides, those with a size outside the expected length of the barcode (<8 and >180 bp) and those represented by only one read in the entire dataset. Taxonomic assignment was performed using the *ecotag* command against multiple reference databases: a comprehensive local database for Mpala Conservancy in Laikipia (11), a partial local database for Gorongosa (5), a grass-specific local database for Serengeti (this study; DNA extracts of vouchers used in (12) were processed following methods described in (5) to create the reference database), and a global reference database generated by in silico PCR from the EMBL database (release 134) using *ecoPCR* (13). We used the *obiclean* command (with parameters $d = 1$ and $r = 0.25$) to detect sequences potentially resulting from PCR and/or sequencing errors. For each PCR product, this program determines if a sequence is more likely to be a true sequence ('head'), a sequence derived from another one ('internal'), or a sequence from which no other sequence is derived and is itself not derived from another ('singleton'). This information was used later in the filtering process to remove probably erroneous sequences. The fasta file was then converted into a sequence-by-sample matrix using the *obitab* command. Additional filtering steps were conducted in R v.3.5.3 (14).

For sites with local reference databases, sequences were preferentially assigned to the local reference database. However, if the assignment score obtained with the local database was <98% and lower than that obtained with the global database, then the sequence was reassigned to the global database. For sites without local databases, sequences were assigned to the global reference database unless the assignment score was higher with one of the local reference databases.

To further curate the dataset, we first discarded PCR products with low numbers of reads. For this, we compared the density distribution of the log-transformed number of reads in controls and in true samples within each library, using the intersection of the two distributions as a threshold. We then removed sequences that were likely to have resulted from PCR or sequencing errors. For this, we first used the outputs of the *obiclean* analysis as follows: for each site and sampling bout, we discarded all sequences that were more frequently considered to be errors (internal) than true sequences (head or singleton) for that site in that year. For sites with local reference databases (Laikipia, Gorongosa, Serengeti), these sequences also needed not to match perfectly with any sequence from the local reference database, or else they were retained. We also filtered out putative contaminants by discarding any sequence that had its maximal average relative read abundance (RRA) in negative controls. Similarly, sequences that displayed low similarity (<80% identity) with their closest match were considered likely to be chimaeras and/or highly degraded sequences and therefore filtered out.

Next, we removed outlier PCR replicates (those with non-reproducible results). For each library, we iteratively determined the density distributions of within- and between-sample distances and discarded replicates that fell within the distribution of between-sample distances, the threshold being defined as the intersection of the two density distributions. This process was iterated until no further replicate was removed. Last, to reduce the impact of low-abundance false positives that can arise from tag-jumps during Illumina sequencing, we removed sequences representing <1% of reads in each sample.

Remaining sequences were considered molecular operational taxonomic units (mOTUs) in subsequent analyses. We refer to mOTUs as 'taxa' throughout the text. Note, however, that the taxonomic identity of an mOTU is not always known beyond the family level (or order, in rare cases), and that taxonomic resolution varies across mOTUs owing to differential discriminatory power of the *trn*L-P6 barcode among plant lineages. For instance, species-level discrimination is limited in some grass lineages where clusters of species share identical barcodes (e.g., PACMAD clade); however, we were nonetheless able to identify most grass mOTUs to species Laikipia, Serengeti, Gorongosa, and Addo—the four most intensively sampled sites and those for which we had local reference databases (3–5). Limitations to taxonomic resolution would not affect our core conclusions about the generality of food-plant partitioning, because clusters of indistinguishable species only reduce the odds of detecting significant dietary differences. However, if resolution is systematically lower for grasses than non-grasses, then it could affect our finding that browsers partition plants more strongly than grazers and our associated inferences about diet breadth (**Fig. S3**) and network structure (**Fig. 5**) as functions of grass RRA. We examined this issue for grasses vs. legumes (the two dominant food-plant families) using our local reference databases for Laikipia and Gorongosa (3–5). Across both sites, we detected 78 grass mOTUs (54 uniquely associated with a single reference sequence, 24 non-uniquely associated with >1 reference sequence) and 68 legume mOTUs (51 unique, 17 non-unique). The mean number of plant species per non-unique mOTU was similar for grasses (3.5) and legumes (2.8). We are thus confident that our results for diet breadth and network structure are qualitatively robust to variation in resolving power.

We used RRA (the proportional abundance of each mOTU per sample) for our analyses. Previous studies show that this approach (*i*) provides a reasonable proxy for consumption in large herbivores

and (*ii*) yields similar inferences to those based on presence/absence data ((4, 5, 15, 16); and see also (17, 18)). One caveat to RRA-based inferences is amplification bias, which can lead to under- or over-representation of sequence reads for certain taxa. For example, sedges (Cyperaceae) are suspected of being underestimated by the *trn*L-P6 approach (19). However, sedges do not account for a large share of plant cover or biomass in African savannas, and this caveat is unlikely to affect our inferences.

Addo samples

The main methodological difference between samples collected in Addo and those from all other sites was the DNA extraction method: whereas we extracted total DNA at other sites, an extracellular DNA-extraction protocol was used for samples from Addo (20). Fresh samples from all ruminants, except buffalo, were collected in tubes containing silica gel and stored dry until DNA extraction in the field. Samples from hindgut fermenters and buffalo were collected in unused plastic bags and kept cool until DNA extraction in the field on the same day. Samples were extracted in the field from a much larger volume of initial material than used at other sites. For this, fecal material was mixed with an equivalent amount of saturated phosphate buffer (Na_2HPO_4; 0.12 M; pH = 8) for 15 minutes to desorb extracellular DNA. DNA extraction followed methods described in (21).

Although the general metabarcoding approach based on the P6 loop of the *trn*L intron and Illumina sequencing was similar for all samples, laboratory steps and data-filtering protocols performed at Université Grenoble Alpes differed slightly from those used at Princeton University. Specifically, the primer pair used was identical to other sites, but the composition of the PCR mix and PCR conditions differed. PCRs were performed in a 20 μL reaction volume containing 10 μL of AmpliTaq Gold 360 master mix (Applied Biosystems), 0.5 μM of each primer, 0.16 μL (20 mg/mL) of bovine serum albumin (BSA, Roche Diagnostic), and 2 μL template fecal DNA extract (diluted 10 times). Polymerase activation was performed at 95ºC for 10 min, followed by 40 cycles of 95ºC for 30 s (denaturation), 50ºC for 30 s (primer annealing), and 72ºC for 60 s (extension), with a final elongation for seven minutes at 72ºC. Three technical PCR replicates were performed. All experiments included extraction controls, blanks, and negative and positive PCR controls. All PCR products (samples and controls alike) were mixed together and purified using the MinElute PCR Purification Kit. Libraries were prepared using the MetaFast protocol (https://www.fasteris.com/dna/?q=content/metafast-protocol-amplicon-metagenomic-analysis) and sequenced in paired-end on a HiSeq 2500 platform (2×150 bp) by Fasteris (Geneva, Switzerland).

Sequence data were processed with *OBITools* software. Paired-end read alignment, assignment of sequences to their original samples, sequence dereplication, removal of sequences with ambiguous nucleotides, and selection of sequences based on their length (range 10–220 bp here) were conducted as described above for the non-Addo sites. In addition, sequences obtained in fewer than two different PCR replicates (with a minimum of 10 reads in at least one of them) were discarded, as were those represented by <100 reads over the entire dataset. The *ecotag* program was used for taxonomic assignment using a comprehensive local reference database for Addo Elephant National Park, comprising 473 plant species. Methods employed to build the reference database followed methods described in Taberlet et al. (22, p. 25), using PCR with the same P6-loop primers. Only sequences with an assignment score ≥0.99 identity were retained. Sequences with >10% of their reads observed in controls were discarded, as were samples with a sequencing depth <2,000 reads after filtering.

We believe that the methodological differences between Addo and other sites are unlikely to severely bias inferences about the proportional representation of different dietary plant families, so we included

Addo data in these analyses (**Fig. 2**). Similarly, although these methodological differences may have caused differences of degree in the analyses of dietary dissimilarity (**Figs. 3, 4**), we consider them unlikely to alter the qualitative pattern of resource partitioning (and the qualitative similarity in results between Addo and other sites bolsters our confidence in this assessment). However, we considered estimates of dietary diversity and plant-herbivore network structure more likely to be sensitive to the differences in extraction protocol and volume of fecal material used, and we therefore excluded Addo from direct comparative analyses of dietary diversity and network metrics (**Fig. 5**).

Confirmation of sample identity

Whenever possible, fecal samples were collected directly after observing animals defecate. In some cases, we were forced to collect samples without a direct observation (e.g., for animals that are most active at night and/or dangerous, such as elephant, rhinoceroses, buffalo, and hippopotamus). We are highly confident of the species assignments used in this study for multiple reasons. First, the collection team always included at least one member with considerable experience in identifying herbivores and their feces. Second, fresh dung is readily distinguishable from even hours-old dung. Third, relatively few sympatric species have dung similar enough to be confused. Fourth, we performed confirmatory analyses whenever we considered it possible that identifications might be mistaken, as detailed below.

We used DNA analyses to confirm the species identity of 200 uncertain samples from 2017-2018. These DNA samples were amplified with tagged primers targeting a 16S metabarcode allowing identification of mammals to species (MamP007F: 5'-CGAGAAGACCCTATGGAGCT-3'; MamP007R: 5'-CCGAGGTCRCCCCAACC-3' (22, 23)). To limit amplification of human DNA, a blocking primer (MamP007_B_Hum1, 5'-GGAGCTTTAATTTATTAATGCAAACAGTACCC3-3' (23)) was added to the mix. PCR amplifications were conducted in a final volume of 20 µL containing 2 µL of template DNA, 0.2 µM of each primer, 2 µM of human blocking primer, 0.2 mM of each dNTP, 0.2 $mg.mL^{-1}$ of BSA, 1X GenAmp Gold II buffer; 2 mM $MgCl_2$, and 1U of AmpliTaq Gold DNA Polymerase. Thermocycling conditions included an initial denaturation at 95°C for 10 min, followed by 35 cycles of denaturing at 95°C for 30s, annealing at 50°C for 30s, extension at 72°C for 30s, and a final elongation step (7 min at 72°C). PCR products were pooled and purified using the MinElute PCR Purification Kit. The library was constructed using a PCR-free protocol and sequenced in paired-end (2×250 bp) on an Illumina MiSeq platform. Data processing was performed with *OBITools*. Paired-end alignment, assignment of sequences to their original sample, dereplication of identical sequences, and removal of low-quality sequences were conducted as described above. We generated a mammal DNA reference database by using in silico PCR from the EMBL database (release 134) to assign sequences to herbivore taxa. PCRs with a low number of reads (<350) were discarded and non-mammalian reads were filtered out. The following criteria were used to define an acceptable assignment: (*i*) >98% similarity (i.e., maximum of 1 bp difference) with a reference sequence, (*ii*) no multiple assignments, and (*iii*) the top sequence was >50% of reads and was at least twice as abundant as the second. In addition, when the identity score was <100%, sequences were manually inspected to check if the barcodes of the putative species were dissimilar enough to avoid misidentification.

A comparable approach was applied to all samples from Addo (2013-2014) using the same primer pair as above. In Laikipia (2013–2016), a barcoding approach based on primer pairs targeting different regions of mitochondrial COI (cytochrome c oxidase subunit I) was used to confirm the identity of 217 of the samples used in the present study (3). In total, we performed confirmatory analyses for 1634 samples of 23 species, encompassing 7 of the 10 sampling sites.

TEXT S2. SUPPLEMENTARY ANALYSIS

Predictors of dietary richness and diversity

Dietary richness and diversity are important descriptors of niche width, but their determinants are poorly understood (5, 24–26). We tested a series of models comprising predictors for which we had biologically based a priori hypotheses (detailed below). We built a candidate set of 16 linear mixed-effects models, including a null model (intercept only) and all additive combinations of 4 fixed effects: (*i*) digestive type (ruminant or non-ruminant), (*ii*) body mass ($\log_e$ transformed), (*iii*) local rainfall (90 d before sampling), and (*iv*) a quadratic proportional grass consumption term (grass RRA + grass RRA^2) as fixed effects; we did not include interaction terms because we had no a priori hypotheses about interactions among the predictors (27). Random intercepts were included for site in all models, and sample size was $n = 119$ population-bouts (**Tables S2 and S3**).

For grass consumption, we selected a quadratic term based on an a priori hypothesis (25), and we also confirmed post hoc that it provided better model fits than a linear term. We included site as a random intercept because we expected herbivore dietary diversity to vary with plant diversity and community composition (we lack vegetation data for the sampled areas at most of our sites), and because several sites were sampled multiple times in different seasons and years. This enabled us to account for effects of site-specific factors, such as plant diversity, while including rainfall (a key determinant of primary productivity that varies temporally within sites) as a fixed effect. We did not include random slopes in part because had no a priori hypothesis about how and why fixed effects should vary across sites (and hence sought to conserve degrees of freedom) and in part because most sites were sampled only once and thus are associated with a single value of rainfall, which precludes estimating site-specific effects. Variance-inflation-factor analysis (in *car* (28)) yielded values < 2, indicating no problematic collinearity between predictor variables. We fit models using maximum likelihood in *lme4* (29) and used the Akaike Information Criterion (AIC_c) to rank models (in *MuMIn* (30)) and calculate the Akaike weight for each model (its likelihood of being the best in the candidate set) and the relative variable importance (RVI, the summed Akaike weights of all models containing that variable) for each fixed effect (27).

Justifications for the fixed effects included in these analyses are as follows:

(1) ***Rainfall.*** Rainfall influences primary productivity (resource availability for herbivores) and plant species composition, and is therefore a likely influence on herbivore diet breadth, although the direction of this effect is not necessarily obvious (higher rainfall might increase dietary diversity if more plant species are available to eat, or it might decrease dietary diversity if herbivores are able to forage more exclusively on a few preferred foods). We used a continuous rainfall variable (total rainfall during the 90 d before sampling) to consume fewer degrees of freedom and to avoid the ambiguity and arbitrariness of a categorical seasonality variable. Some of our sites have unimodal rainfall distributions (e.g., Gorongosa, Nyika) while others have weakly seasonal or multi-modal rainfall distributions (e.g., Laikipia, Addo); our southern sites have more pronounced temperature seasonality than those closer to the equator; our sampling did not always fall squarely within a categorical season; and there are often marked differences in plant attributes within seasons (e.g., between early and late dry seasons in sites with unimodal rainfall) (see **Table S1** for site attributes).

(2) ***Body size.*** Multiple arguments from first principles, as well as some empirical data (31), suggest that larger-bodied herbivores should have more diverse diets (but see (25, 26)). Larger herbivores require more forage biomass and tend to range over larger areas, both of which might lead to the ingestion of a larger number of plant species (32, p. 4). It has also been hypothesized that larger-bodied herbivores are more rate-limited in their ability to detoxify plant secondary compounds

(which tend to be species- or lineage-specific and dosage-dependent) and thus need to diversify their diets to avoid overdosing on any given compound (25).

(3) ***Digestive type.*** Similar arguments suggest that nonruminants should have broader diets than ruminants: hindgut fermenters eat comparatively larger quantities of lower-quality forage (33). To the extent that detoxification limitation promotes dietary diversification, hindgut fermenters might also be more affected, because the ruminant microbiome facilitates detoxification (34). A previous study from Laikipia (25) found modest support for digestive type (after proportional grass consumption) in predicting dietary diversity, although there diversity trended higher in ruminants.

(4) ***Quadratic proportional grass consumption.*** We used a quadratic term for grass consumption (grass RRA + grass RRA^2) because (*i*) previous work (25) showed that dietary diversity was a hump-shaped function of proportional grass consumption (and that the quadratic term strongly outperformed the linear term in predicting dietary richness, diversity, and evenness); and (*ii*) mixed feeders should have more diverse diets than strict browsers or grazers because mixed feeders eat substantial quantities of both monocots and eudicots, which broadens potential diet breadth (35).

For both dietary richness and diversity, the model with quadratic grass RRA alone was the single best fit (marginal r^2 = 0.26 and 0.16, conditional r^2 = 0.37 and 0.16, Akaike weights = 0.35 and 0.29, respectively; **Fig. S3**, **Tables S2 and S3**). For dietary richness, one additional model had substantial empirical support ($\Delta AIC_c < 2$), which included grass RRA and body mass (with positive coefficient, indicating that diet breadth trended higher in large-bodied species); for dietary diversity, two additional models had $\Delta AIC_c < 2$, and these paired grass RRA with rainfall (diet breadth trended higher with increasing rainfall) and digestive type (diet breadth trended higher in ruminants). The RVI of quadratic grass RRA was 1.00 for both dietary richness and diversity, indicating that all empirically supported models contained this term. By contrast, all other predictors had RVI ≤ 0.41. Thus, we found at most marginal support for the prediction that diet breadth is greater in larger-bodied species (body mass RVI = 0.37 and 0.25), in non-ruminants (RVI = 0.26 and 0.31, with the direction of the effect contrary to our prediction), or at high rainfall (RVI = 0.25 and 0.41). These results mirror site-specific findings from Laikipia, showing that the hump-shaped pattern of diet breadth along the grazer-browser spectrum (and the limited effect of body size and digestive morphology), is upheld across diverse savannas. These results are also consistent with a global macroecological analysis showing no trend in dietary generalization with body size among vertebrate herbivores (26).

Future work can build on our results by incorporating additional data on local ecological context to predict dietary diversity. For example, although rainfall had limited explanatory power in our models, data on locally available plant biomass and community diversity would enable deeper insight into environmental constraints on diet breadth. Fine-grained vegetation data would also enable calculation of selectivity indices (use relative to availability) to inform interpretation of patterns in dietary diversity. Previous studies have used DNA-metabarcoding data to estimate selection by giraffe for tree species in Laikipia (26) and by 6 ungulate species for understory plants in Gorongosa's Lake Urema floodplain (5), although it is more difficult to quantify the availability of both understory and overstory plants in a common currency (36). Future work might also consider interactions among predictor variables. We followed best practice in model selection by omitting interactions, for which we had no a priori ecological hypotheses (27), but exploratory post-hoc analysis revealed potential interactions between body mass and digestive type for (a) grass RRA (decreased with size in non-ruminants, increased marginally with size in ruminants) and (b) dietary richness (increased with size in non-ruminants, no trend in ruminants). Parsing these relationships (and distinguishing the effects of body mass per se from those of species identity and phylogenetic relatedness among the limited number of non-ruminant species sampled here) is beyond the scope of the present study but merits further attention.

Predictors of pairwise niche differentiation

We used the same model-selection approach to analyze the r^2 from the 723 pairwise perMANOVA of dietary dissimilarity between sympatric species within the same sampling bouts (**Dataset S25**). These r^2 values measure the variance in dietary dissimilarity explained by herbivore species identity alone (**Fig. S10B**) and are strongly positively correlated with the raw Bray-Curtis dissimilarity index (r = 0.50). However, Bray-Curtis values have a heavily skewed distribution and are sensitive to unbalanced sample sizes and differences in dispersion between species, whereas the r^2 values are normally distributed (1^{st}–99^{th} percentiles 0.05–0.60, mean and median 0.30) and are based on species' centroids.

Our candidate model set paralleled that used for diet breadth above, with a similar rationale. As above, site was included as a random intercept in all models to account for the multiple sampling bouts within several sites and any context-dependent variation unrelated to rainfall (which was included as a fixed effect). Because the response variable pertains to the difference between each unique pair of sympatric species, the remaining fixed effects were calculated as differences. For each species pair, we calculated $\log_e$ difference in body mass (Δbody mass); digestive system (Δdigestive system, a categorical variable with 3 levels, nonruminant vs. nonruminant, nonruminant vs. ruminant, and ruminant vs. ruminant); and grass RRA (Δgrass RRA). The rationale for the choice of fixed effects in this analysis is as follows:

(1) ***Rainfall.*** We included rainfall (90 d prior to sampling) to test the prediction that niche differences are stronger when food is limited. Aboveground plant biomass in savannas is tightly correlated with rainfall, and food for herbivores is accordingly most limited during dry periods (37).
(2) **Δ*Body mass*.** We included this term to test the prediction that diet differentiation is stronger between species of divergent size, which have corresponding differences in both nutritional requirements (38) and ability to access and process plants with different traits (39).
(3) **Δ*Digestive system*.** We included this term to test the prediction that species with similar gut morphology eat similar diets. Ruminants and nonruminants have different digestive capacities and constraints that may translate into differences in dietary species composition. Rumination enables thorough digestion but limits intake rate, suggesting that ruminants may tend to feed on more nutritious plant taxa; hindgut fermentation is less thorough but throughput is higher, suggesting that nonruminants may tend to feed on fibrous plant taxa with lower mean nutritional quality (33).
(4) **Δ*Grass RRA*.** We included this term because it is a trivial covariate of dietary dissimilarity that we sought to control for in testing the other predictors; dietary differences will inherently be stronger between species on opposite ends of the grazer-browser spectrum (r^2 = 0.25; **Fig. S11D**), and we wanted to evaluate effects of rainfall, body mass, and digestive type after accounting for this effect.

Pairwise comparisons between species should be independent of extrinsic factors such as the number of other species sampled at a site; all else equal, any randomly drawn pair of species at a site should be as likely to have similar diets (e.g., two grazers) as to have dissimilar ones (e.g., a grazer and a browser). We therefore decided a priori not to include sampling coverage as a predictor. However, we found that the 3 highest r^2 values occurred at sites with low sampling coverage (Hwange with 5 species and two bouts in Kruger with 3 species each), raising the prospect that poorly sampled assemblages might have artificially inflated estimates of niche differentiation. To test this possibility, we first regressed the mean r^2 for each site and bout against the number of species sampled in that bout (as per **Fig. S10B**), which revealed no correlation (r^2 = 0.004, $F_{1,22}$ = 0.098, p = 0.76). We next conducted a more liberal analysis, regressing the r^2 of all 723 pairwise perMANOVA against the number of species sampled in the corresponding bout for each pair. This revealed an extremely weak (r^2 = 0.008) albeit statistically significant ($F_{1,721}$ = 5.85, p = 0.02) *positive* trend. Thus, if anything, there was a very marginal tendency to observe stronger niche differences at more extensively sampled sites, meaning that under-sampling an assemblage is (if anything) conservative with respect to our inferences about the generality

of food-plant partitioning. In light of these post-hoc analyses, and lacking any convincing biological or statistical explanation for the existence of a real relationship between these variables, we decided not to retroactively update our candidate-model set to include sampling coverage as a predictor.

The results are summarized in the main text and detailed in **Table S4**; to assist intuition, we also show one-way relationships between the response and each predictor (**Fig. S11**), but our inferences are based the mixed-effects models that include random intercepts for site. The top model (marginal r^2 = 0.27, conditional r^2 = 0.54, Akaike weight = 0.56) included Δbody mass (RVI = 1.00) and rainfall (RVI = 0.65) in addition to Δgrass RRA; the coefficients of Δbody mass (positive) and rainfall (negative) were in accordance with our predictions. The 2nd-ranked model (ΔAIC_c = 1.22, weight = 0.31) included only Δbody mass and Δgrass RRA, and the 3rd- and 4th-ranked models (ΔAIC_c = 3.85 and 4.99, weights = 0.08 and 0.05) paired the top two models with Δdigestive system (RVI = 0.13). This last predictor was the only one that countered expectation; diet differences were if anything strongest between pairs of nonruminants (**Fig. S11C**).

These 723 pairwise contrasts included 89 pairs (from 5 sites) in which $n < 10$ for one or both species, but results were qualitatively equivalent (indeed marginally stronger with respect to our predictions) when we analyzed just the 634 contrasts with $n \geq 10$ for both species; the rank ordering of the top 4 candidate models (all those with ΔAICc < 23 and Akaike weight > 0.005) was identical to that in **Table S4**, as was the ordering of the bottom 8 models. The results were also unaffected when we analyzed Δdigestive system as a binary variable (1 = different gut type, 0 = same gut type) instead of a 3-level categorical variable.

Future work incorporating site-specific attributes such as local species richness and relative availability of plant taxa would enable deeper mechanistic insight into the drivers of dietary differentiation. One outstanding question is the relative extent to which differences in diet composition reflect fine-grained differences between herbivore species in space use vs. selectivity/preference for plant taxa. Given the universality of pairwise differences in diet composition (**Dataset S25**), the answer is almost certainly both, because our study includes pairs of species that routinely co-occur side by side (often foraging within the same mixed groups) in addition to species with well documented differences in habitat affiliation. Moreover, to the extent that sympatric species segregate at fine spatial scales, these differences may themselves be driven by differences in selectivity and/or competitive ability for particular plant taxa, making the proximate behavioral and cognitive bases of dietary differentiation hard to parse in the absence of cafeteria-style choice experiments (which are unwieldy given the diversity of plant and herbivore species, but could be applied for salient focal comparisons). Because we sought mainly to establish the generality of food-plant partitioning and were unable to account for fine-scale variation in plant community composition and herbivore space use at the broad spatial and temporal scales required to do that, we explicitly assumed that sampling over relatively small areas would increase the likelihood that plant relative availability would be comparable for all species (**Fig. S1**); in this case, differences in diet composition should equate to differences in selectivity. However, we acknowledge the possibility that this assumption was not valid in all cases and encourage any attempts to prove that. The increasing ability to monitor herbivore movements using GPS telemetry and diets using DNA metabarcoding presents exciting opportunities to combine explore the relationship between space use and food-plant selection.

SUPPLEMENTARY FIGURES

Figure S1. Sample-collection locations (crosses with species-specific colors) at the study sites. We concentrated our sampling effort over relatively small areas at each site (median sampling area per site = 194 km^2, equivalent to a square with 14-km sides). Within these small areas, we further attempted to sample species evenly and with as much interspersion as possible to minimize confounding effects of spatial segregation and large-scale gradients in the availability of different plant taxa; we likewise sampled species during short, within-season sampling bouts to minimize any effects of temporal variability. Owing to these spatiotemporal limits and interspersion, we assumed that all sampled herbivore species had access to the same plant communities, meaning that differences in diet composition should reflect differences in selectivity (use relative to availability) for different plant taxa (see **Text S2**). Maps at left in each panel **(A–I)**, corresponding to each site in order from north to south, show the sampling area within each national park or geographic region; maps on the right are magnified views of the sampling area. Axes show latitude and longitude. Samples from all bouts (seasons and years) at each site are shown together. We omit rhinoceros sampling points to avoid jeopardizing the rhinoceroses. For each site, we report the range of minimum convex polygon (MCP) areas encompassing 95% of sampling points (to exclude outlying samples and any GPS errors) in each sampling bout (these values are also in **Table S1**) along with the cumulative MCP area encompassing all samples and bouts. Accurate GPS data for Hwange National Park were not available but the sampling area was comparable in size to other sites.

A. Laikipia, Kenya (2013–2016). Samples were collected at Mpala Research Centre and Conservancy (central outline in the left-hand map) and the neighboring Ol Jogi Conservancy. MCP range = 68–151 km^2, cumulative MCP = 194 km^2.

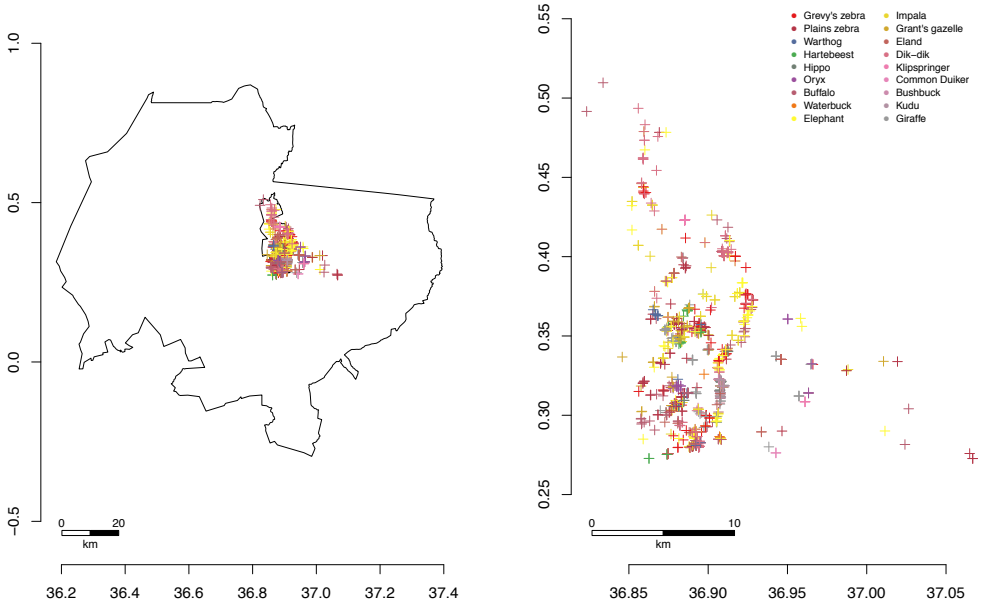

B. Serengeti National Park, Tanzania (2017–2018). MCP range = 267–835 km^2.

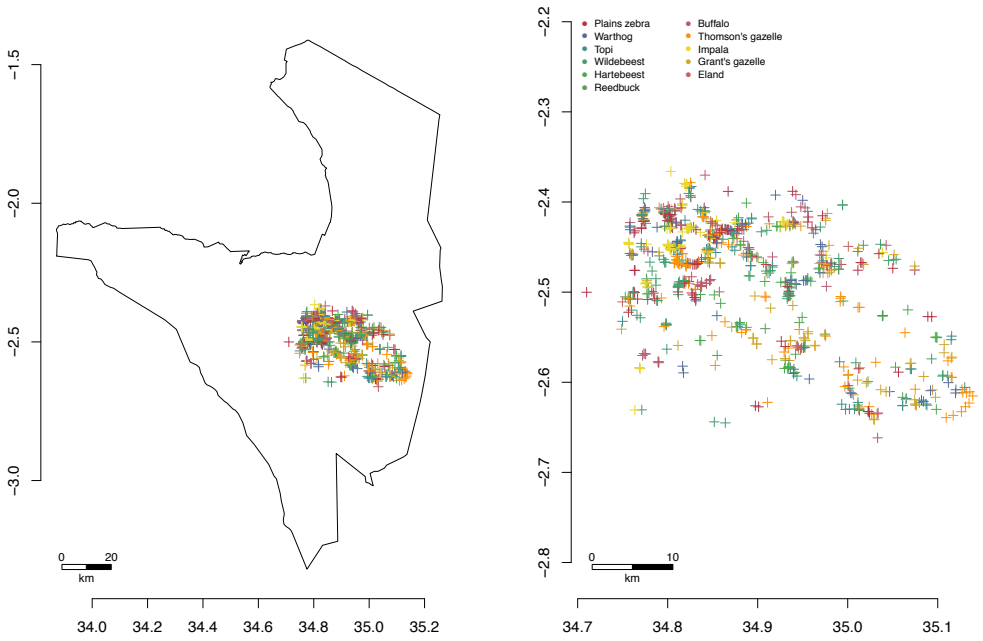

C. Nyika National Park, Malawi (2017). MCP = 352 km^2.

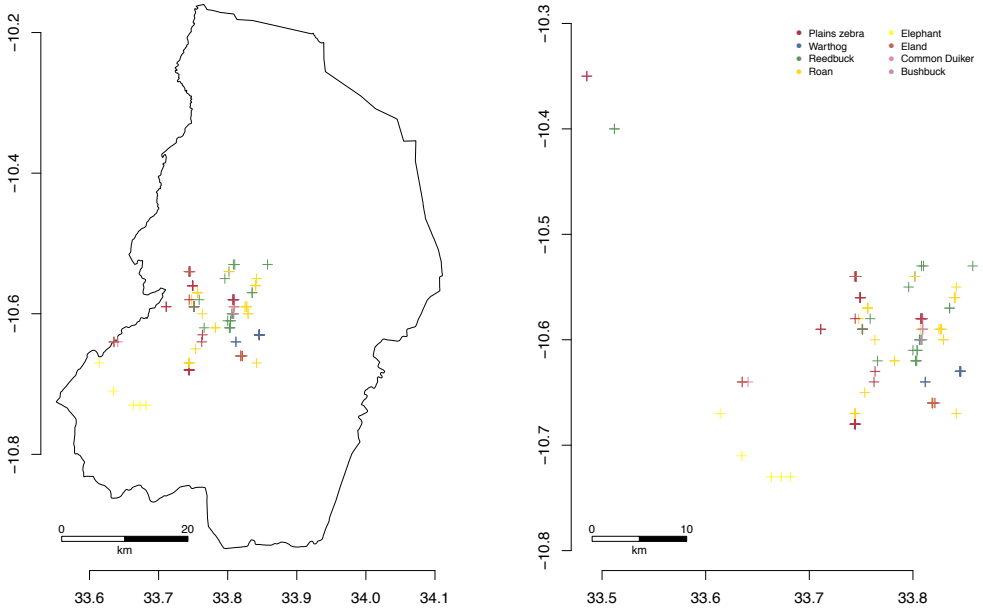

D. Niassa National Reserve, Mozambique (2017). MCP = 149 km^2.

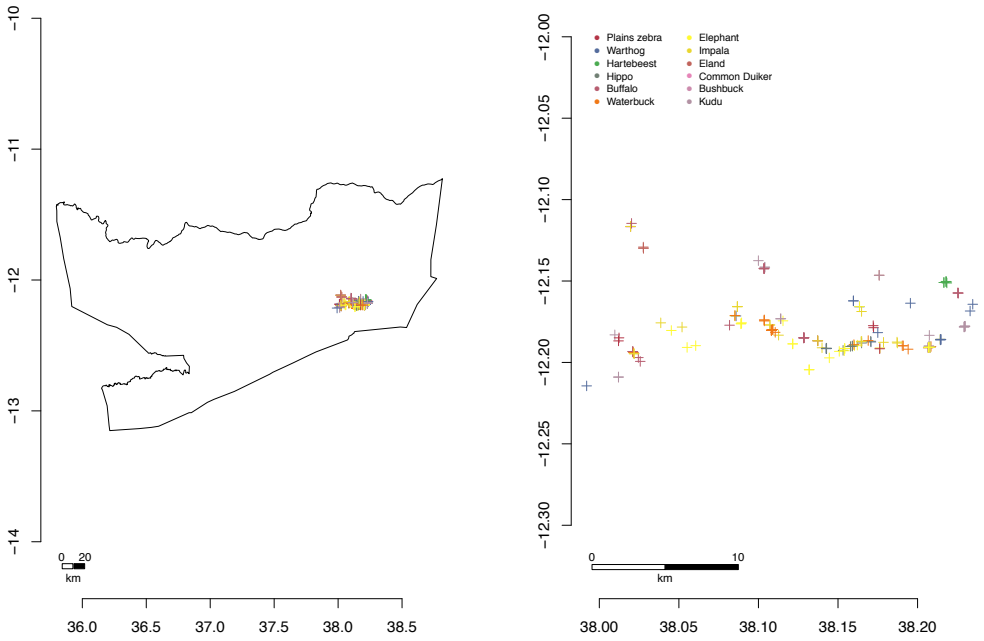

E. Kafue National Park, Zambia (2017). MCP = 61 km^2.

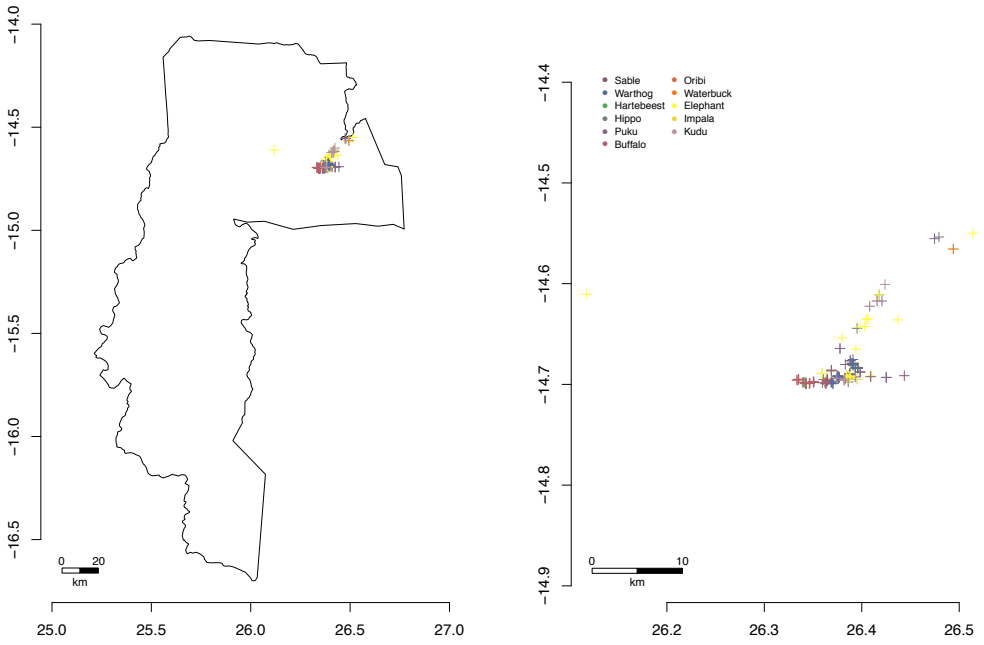

F. Gorongosa National Park, Mozambique (2016–2017). MCP range = 49–350 km^2, cumulative MCP = 321 km^2.

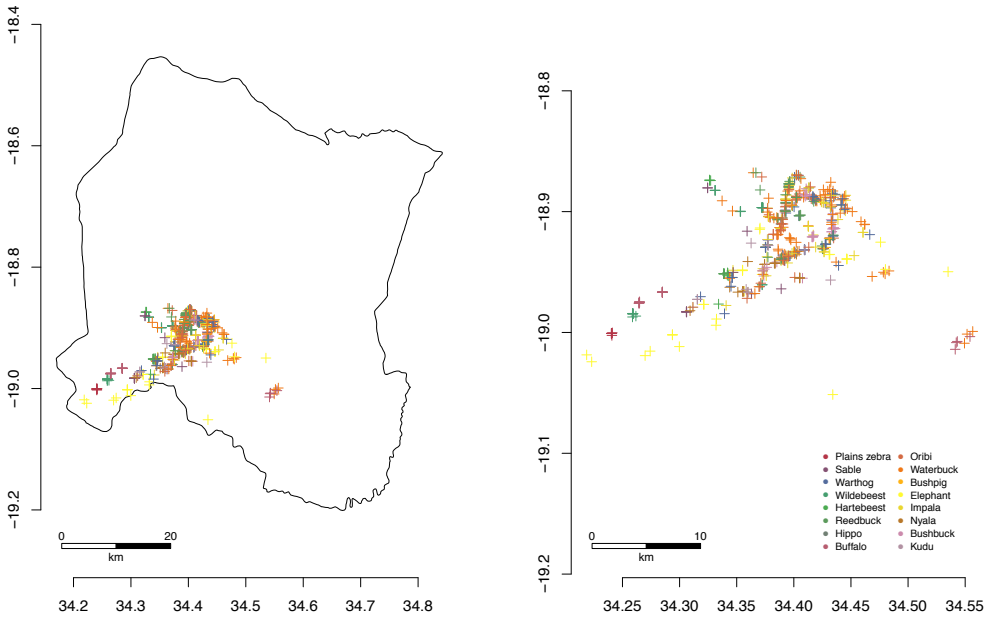

G. Kruger National Park, South Africa (2017). MCP range per sampling bout= 9–20 km^2, cumulative MCP = 30 km^2.

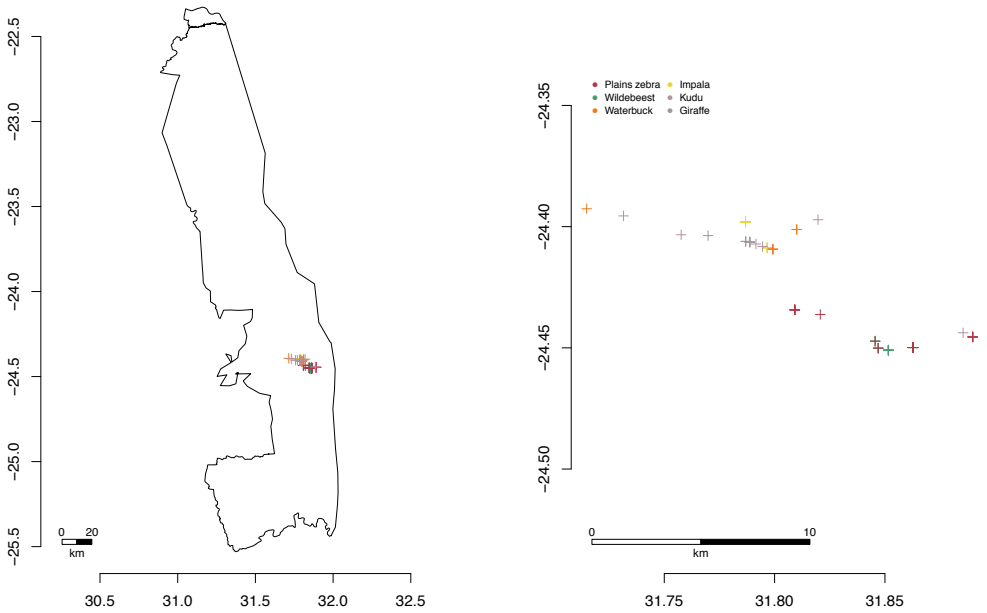

H. Hluhluwe-iMfolozi Park, South Africa (2017). MCP = 370 km^2.

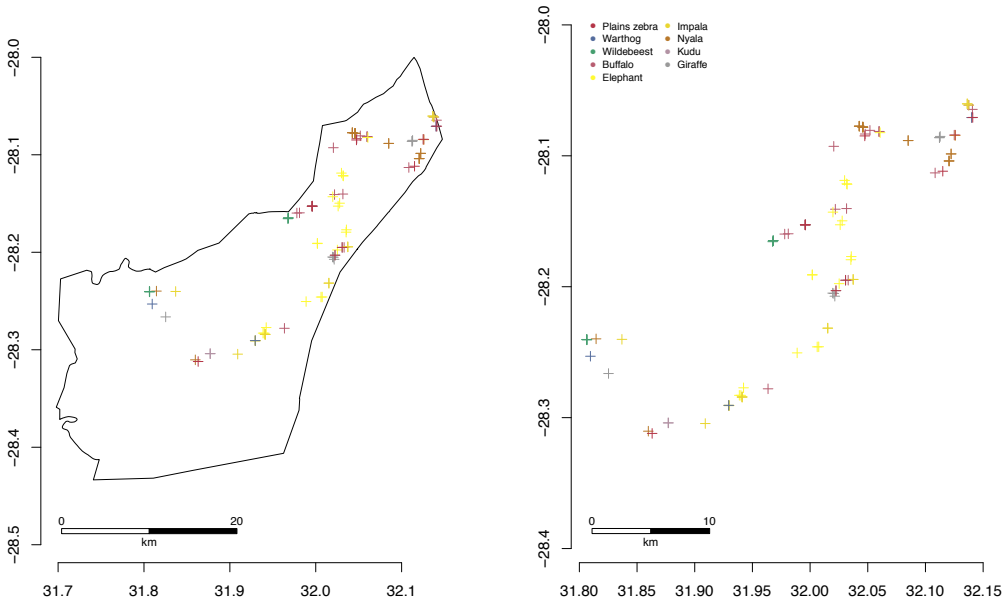

I. Addo Elephant National Park, South Africa (2013–2014). MCP range per sampling bout = 22–49 km^2, cumulative MCP = 47 km^2.

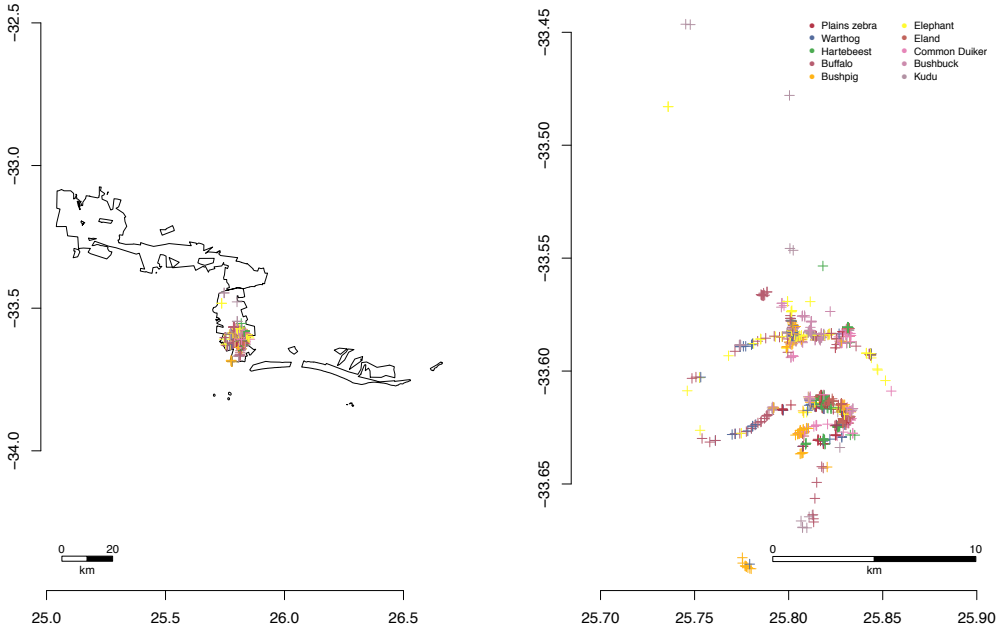

Figure S2. Population- and assemblage-level dietary richness. Colored dots show the rarefied population-level dietary richness (number of food-plant mOTUs) for each herbivore species in each site and sampling bout (including only bouts where ≥5 herbivore populations were represented by ≥10 samples, and excluding Addo owing to the methodological differences described in **Text S1**). Population-level dietary richness was calculated by randomly resampling to a common depth of 10 samples and averaging across 100 iterations. Grey bars show the rarefied dietary richness of the assemblage after randomly resampling to 10 samples per species; numbers above bars are the number of species sampled. Although assemblage-level dietary richness should in general be an increasing function of the number of species sampled, there was no significant association across these 13 bouts ($r^2 = 0.16$, $F_{1,11} = 2.07$, $P = 0.18$). The median herbivore population ate ~30% of the food-plant taxa consumed by the median assemblage in any given bout.

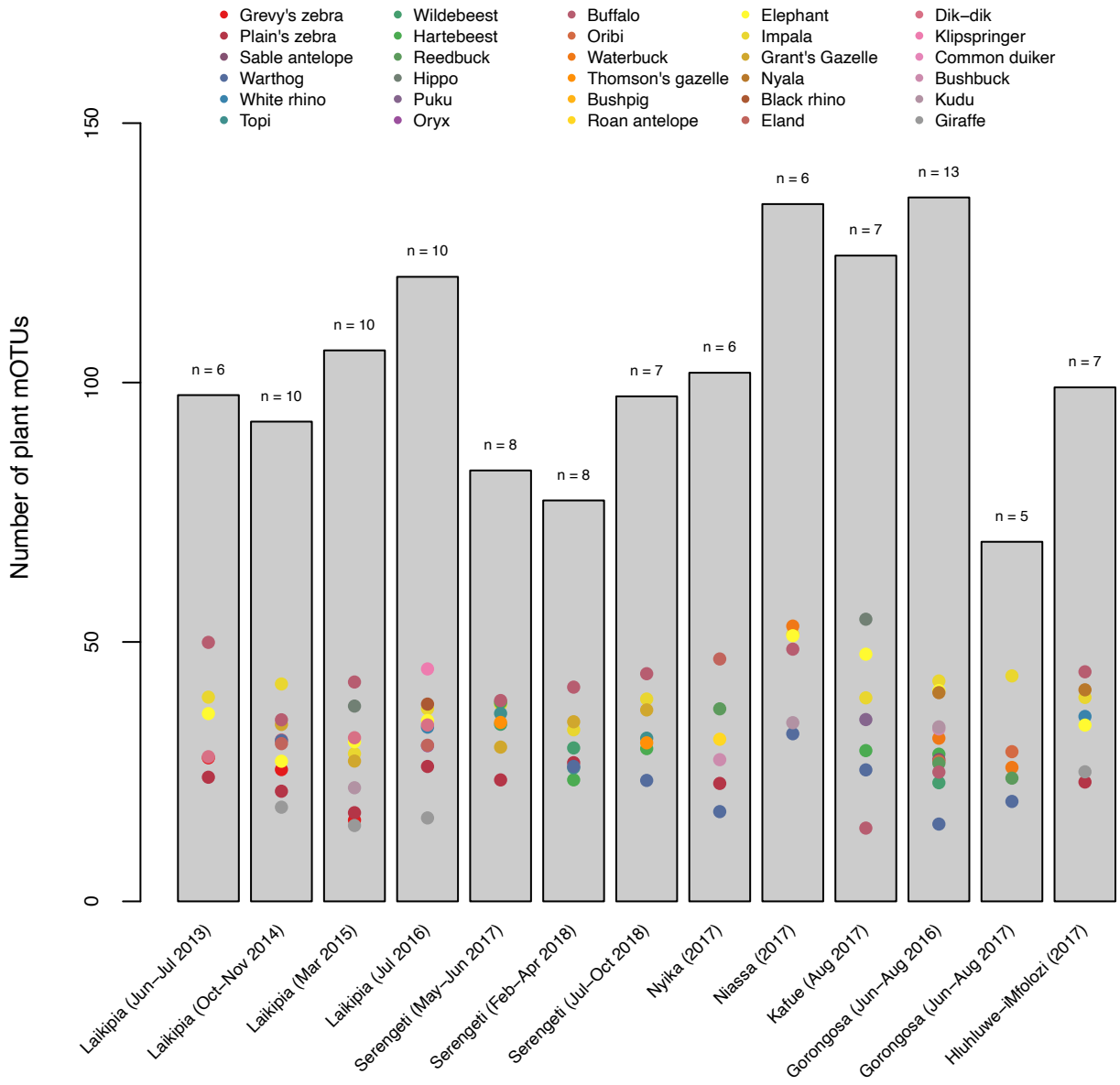

Figure S3. Population-level dietary richness and diversity as functions of grass consumption. **(A)** Population-level dietary richness (number of plant mOTUs) and **(B)** dietary diversity (Shannon index) as functions of mean grass RRA in the fecal samples of each herbivore population (open markers, colored according to site) in each sampling bout at each of the 7 best-sampled sites (excluding Addo owing to methodological differences and Hwange and Kruger owing to insufficient sampling). Diversity metrics were calculated by iteratively rarefying the data for each population to 10 samples and taking the average of 100 iterations. Colored curves are quadratic regressions (diet breadth ~ grass RRA + grass RRA^2) for each sampling bout (solid, $p \leq 0.10$; dashed $p > 0.10$) and show the qualitative similarity across sites, although the small number of species per site (median 7) compromises the power for site-specific statistical testing. Thick curves with shaded 95% CIs are quadratic regressions across all populations and sampling bouts ($n = 119$), corresponding to the top-ranked models for dietary diversity (whole-model $F_{2,116} = 10.53$, $p < 0.0001$, $r^2 = 0.15$) and richness (whole-model $F_{2,116} = 22.81$, $p < 0.0001$, $r^2 = 0.28$), but here without the random effect of site (see **Tables S2 and S3**).

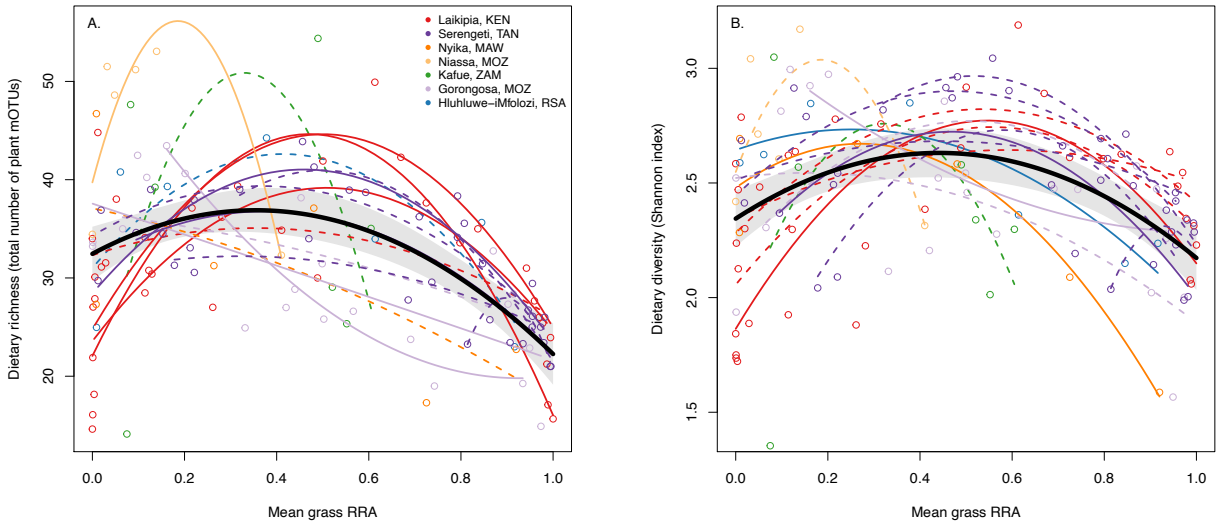

Figure S4. Distribution of populations and species along the grazer-browser spectrum. Histograms show the frequency of proportional grass consumption (grass RRA) among **(A)** species (n = 30), averaging across all sites and sampling bouts, and **(B)** geographically separated populations (n = 90), averaging across bouts for populations sampled repeatedly at a given site; only populations with $n \geq 10$ samples per bout are included. These 'J-shaped' bimodal distributions qualitatively match those obtained by other methods in a recent synthesis of diets from 100 extant large mammalian herbivore species in Africa (40), albeit with a generally higher frequency of populations and species falling in between the two extremes.

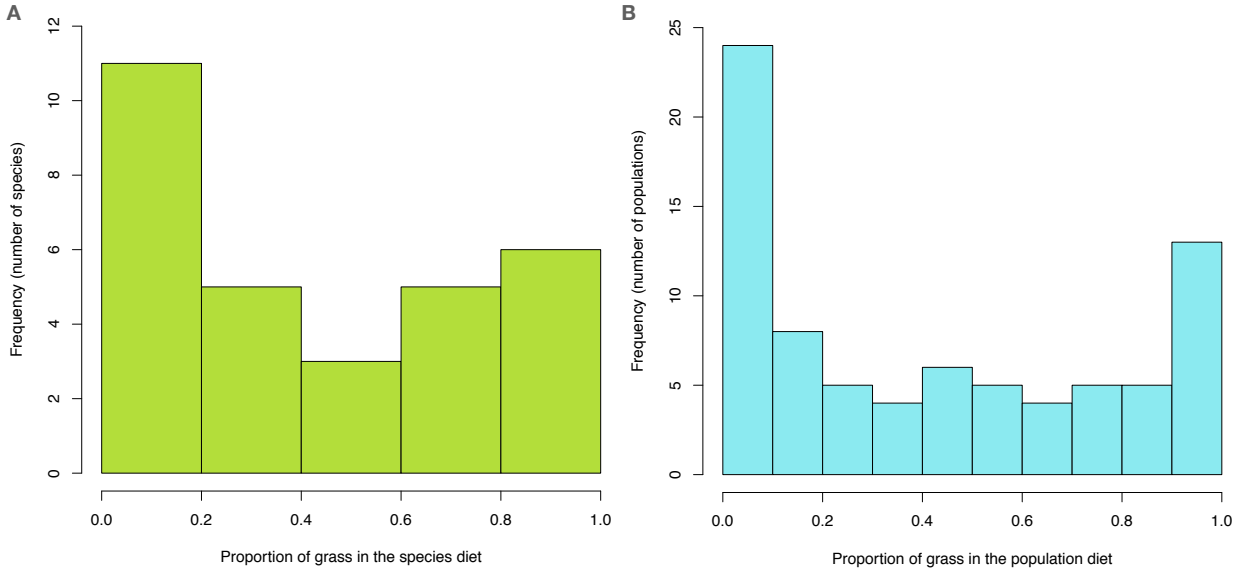

Figure S5. Grass consumption by populations and assemblages as functions of recent rainfall. **(A-E)** Mean grass RRA for the five most extensively sampled species (represented by ≥8 sampling bouts from ≥4 sites) as functions of rainfall during the 90 d preceding sample collection. Marker colors show site. **(A)** Plains zebra, **(B)** warthog, **(C)** buffalo, **(D)** elephant, **(E)** impala. **(F)** Mean grass RRA of entire sampled assemblages at the 7 best-sampled sites, excluding Addo. All panels include only populations represented by ≥ 10 samples per bout. We evaluated linear, exponential, logistic, and log-log fits for each regression, adding 0.00001 to each rainfall value to eliminate the zeroes for Niassa and Kafue; only the best fit is shown. Trendlines (solid, $p \leq 0.10$; dashed, $p > 0.10$) are log-log fits for each panel except impala (E), where exponential regression fit better. While the trend in all panels is positive, it is generally weak and heavily influenced by the outlying low values of rainfall in Niassa and Kafue; the scatter in these relationships suggests that factors other than rainfall influence the observed variability in grass consumption.

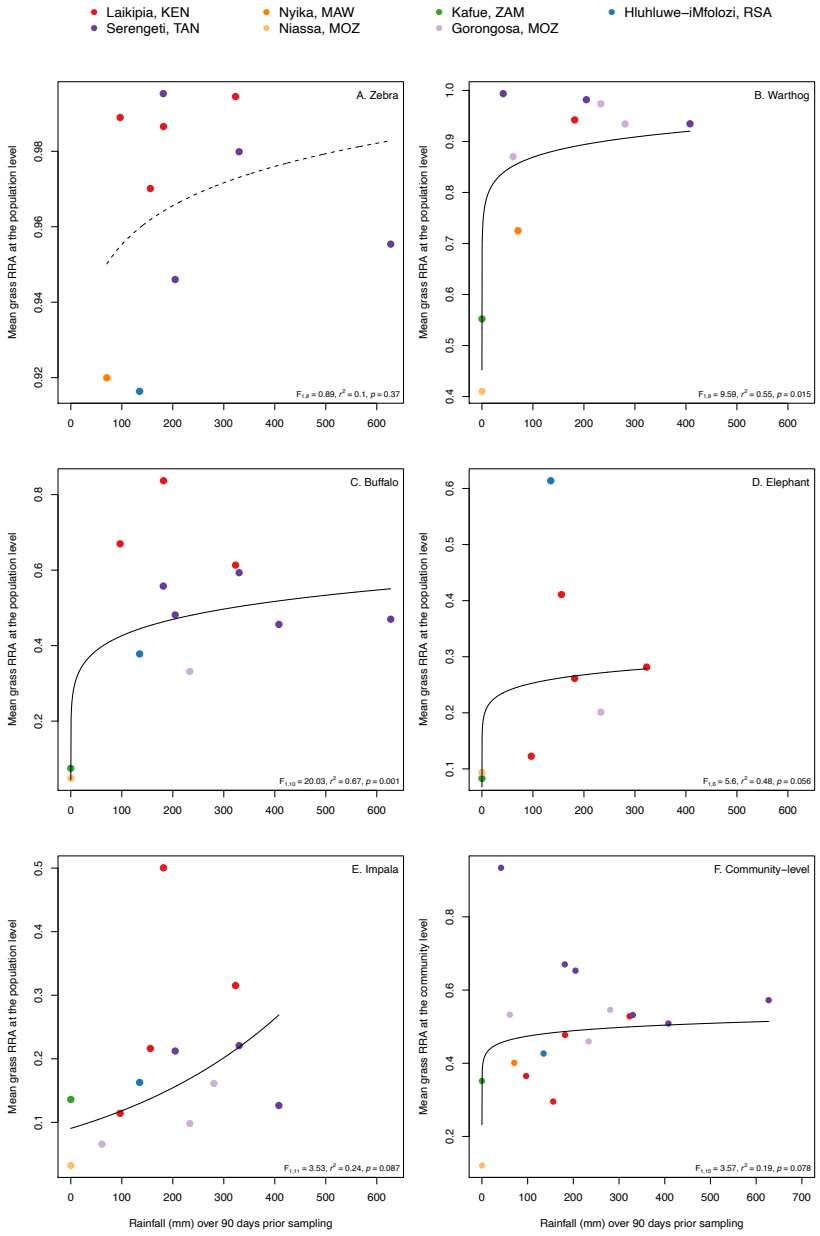

Figure S6. Assemblage-level dietary dissimilarity for all bouts at the repeatedly sampled sites. This presentation is analogous to **Fig. 3** in the main text. **(A)** Laikipia, Kenya; **(B)** Serengeti National Park, Tanzania; **(C)** Gorongosa National Park, Mozambique; **(D)** Kruger National Park, South Africa; **(E)** Addo Elephant National Park, South Africa. Each graph shows the NMDS ordination for a given sampling bout; ellipses show 1 SD. To maximize information content in these supplementary analyses, we relaxed the sample-size threshold used for our main analyses (n = 10 samples per bout) to n = 8 for Laikipia, Serengeti, and Gorongosa and n = 6 for Kruger (species included by virtue of relaxing the sample-size threshold are listed in the heading of each panel). Stress value and permutational analysis of variance (perMANOVA) testing for significant differences among species are shown in each graph. Each panel specifies the month range of the sampling bout and our best attempt to categorize the season; rainfall in the 90 d preceding each bout and the mean annual precipitation for each site are in **Table S1**.

S6A. Laikipia, Kenya. Sample-size threshold was relaxed for hartebeest and kudu in 2014 (n = 8); for hartebeest in 2015 (n = 8); and for buffalo, Grevy's zebra, and warthog in 2016 (n = 8–9).

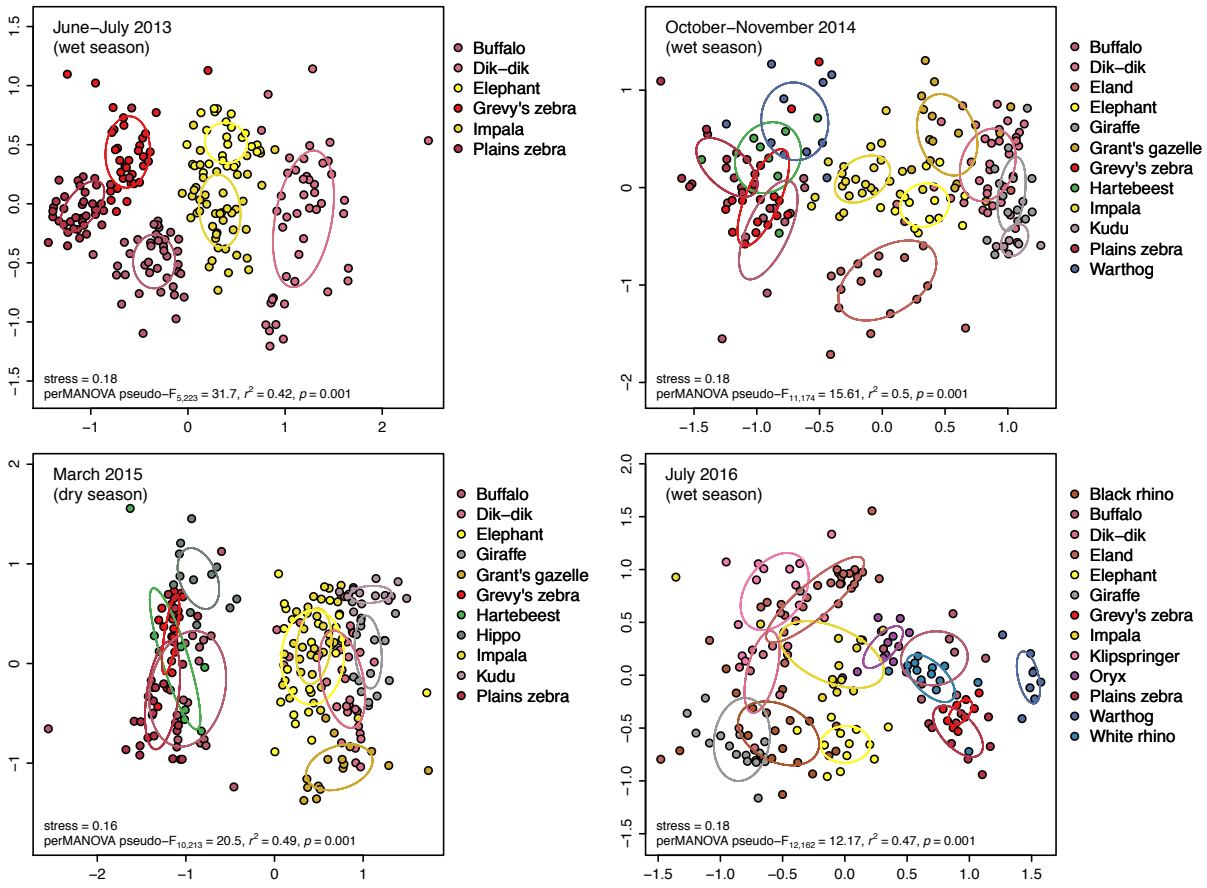

S6B. Serengeti National Park, Tanzania. Sample-size threshold was relaxed for warthog in December 2016–February 2017 (n = 8); for Grant's gazelle, impala, plains zebra, and topi in August–October 2017 (n = 9); and for impala, topi, and warthog in May–June 2018 (n = 8–9).

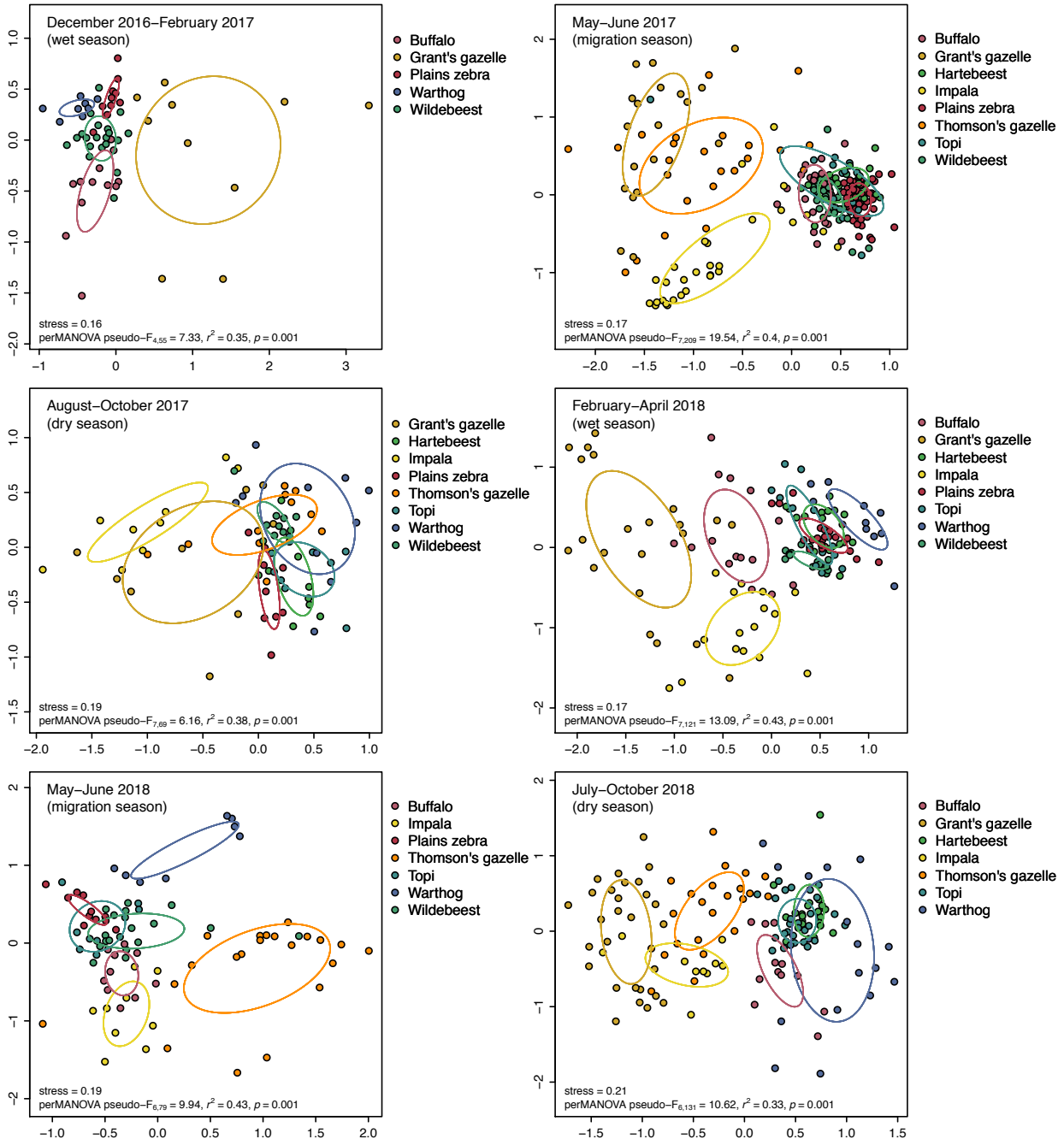

S6C. Gorongosa National Park, Mozambique. Sample-size threshold was relaxed for waterbuck in October–November 2017 (n = 9).

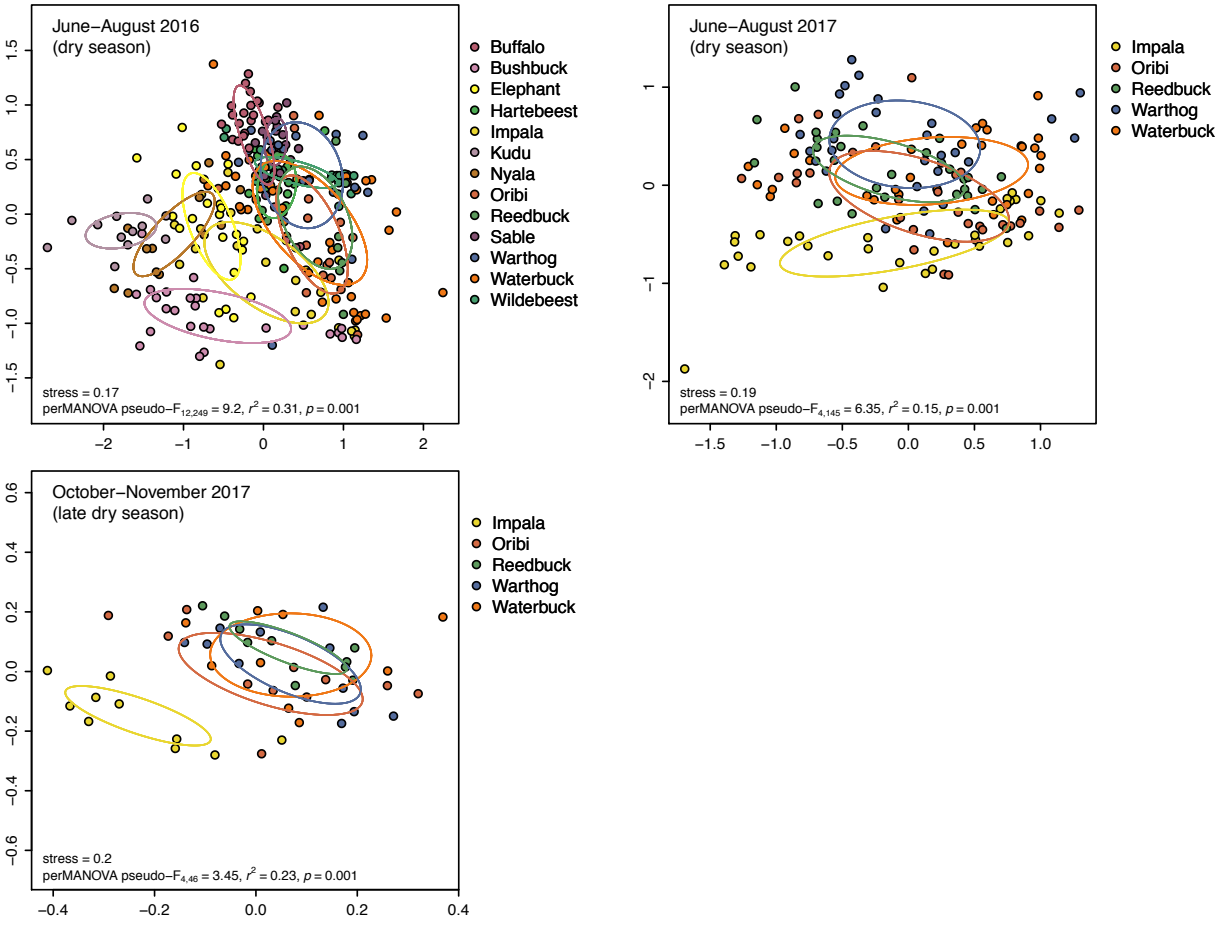

S6D. Kruger National Park, South Africa. Sample-size threshold was relaxed for the 3 species sampled in October 2017 (n = 6 for giraffe and waterbuck, n = 7 for kudu).

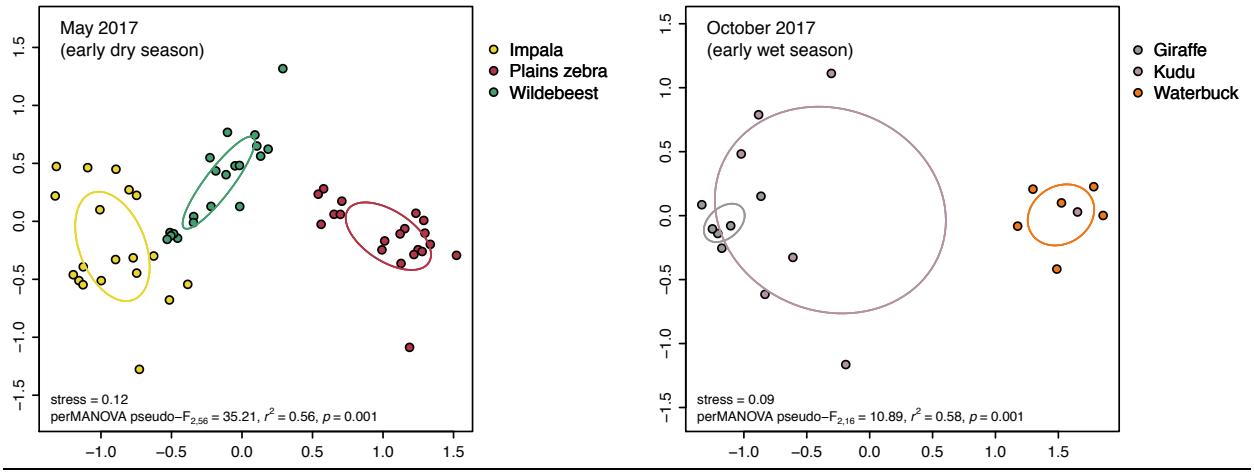

S6E. Addo Elephant National Park, South Africa. All species represented by $n \geq 10$ samples per bout.

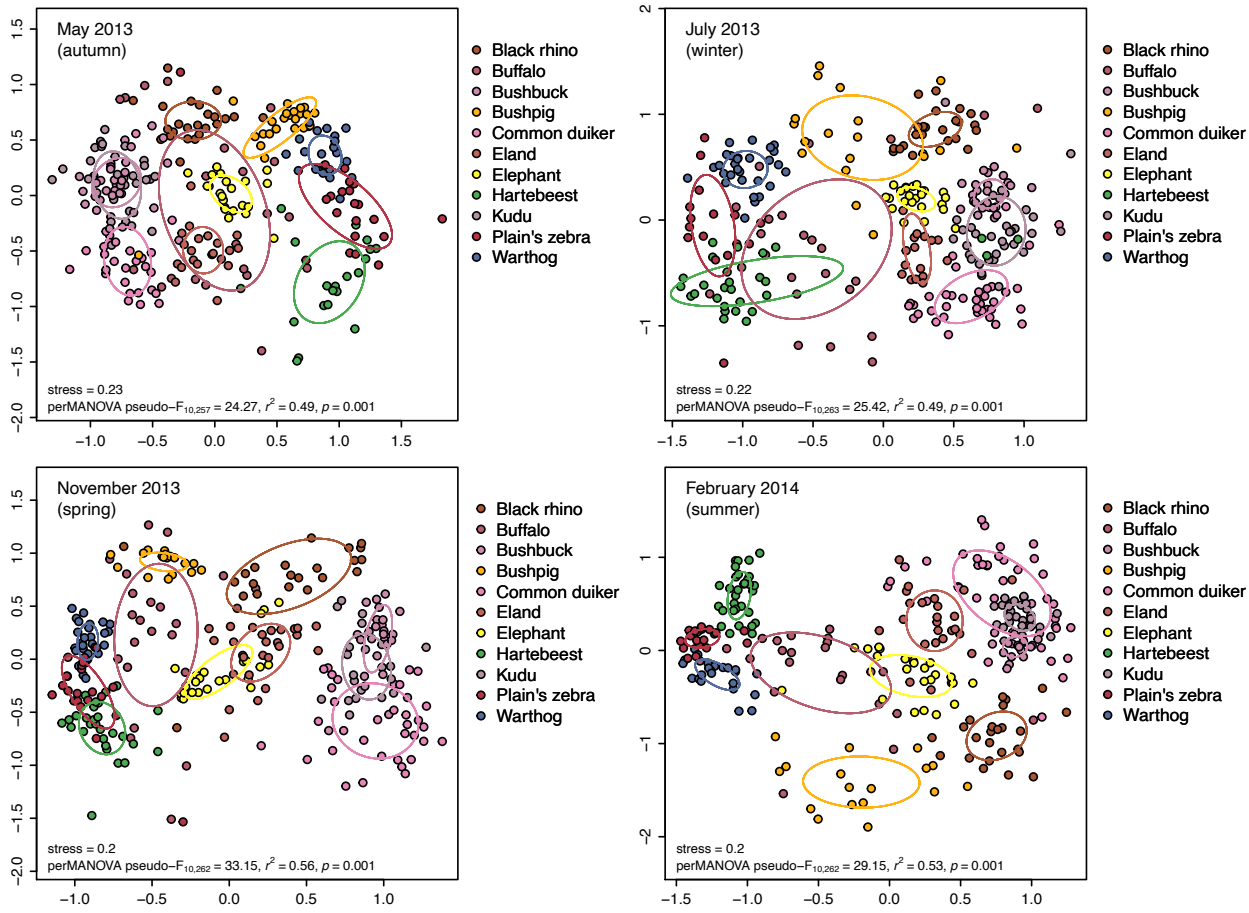

Figure S7. Ordinations of dietary dissimilarity for the strictest browsers (triangles) and the strictest grazers (diamonds and circles) in each sampling bout at the repeatedly sampled sites. This presentation is analogous to **Fig. 4** in the main text. **(A)** Laikipia, Kenya; **(B)** Serengeti National Park, Tanzania; **(C)** Gorongosa National Park, Mozambique; **(D)** Addo Elephant National Park, South Africa. Each graph shows the NMDS ordination for a given sampling bout; species are those with the lowest mean grass RRA (browsers) and highest mean grass RRA (grazers) in that bout. To maximize the number of within-guild contrasts in these supplementary analyses, we relaxed the sample-size threshold used for our main analyses (n = 10 samples per bout) to n = 8 (species included by virtue of relaxing the sample-size threshold are listed in the heading of each panel). Stress value and permutational analysis of variance (perMANOVA) testing for significant differences among species are shown in each graph.

S7A. Laikipia, Kenya. Sample-size threshold was relaxed for kudu in 2014 (n = 8) and warthog in 2016 (n = 8).

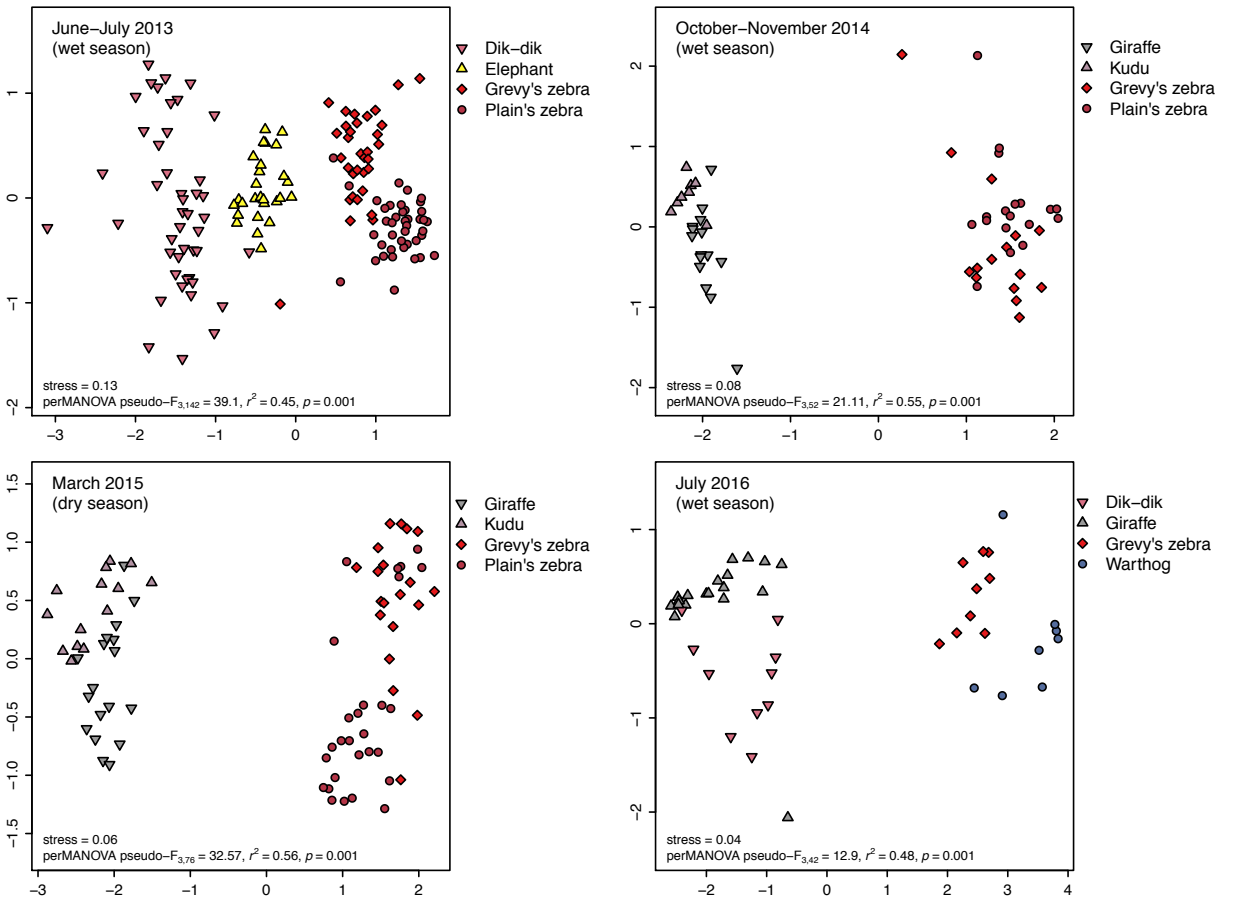

S7B. Serengeti National Park, Tanzania. Sample-size threshold was relaxed for warthog in December 2016–February 2017 (n = 8); for Grant's gazelle, impala, and topi in August–October 2017 (n = 9); and for impala and warthog in May–June 2018 (n = 8–9). Buffalo and Thomson's gazelle were among the species with the most browse-based diets in at least one of these sampling bouts, despite their common categorization as grazers (see **Fig. 2A–C**).

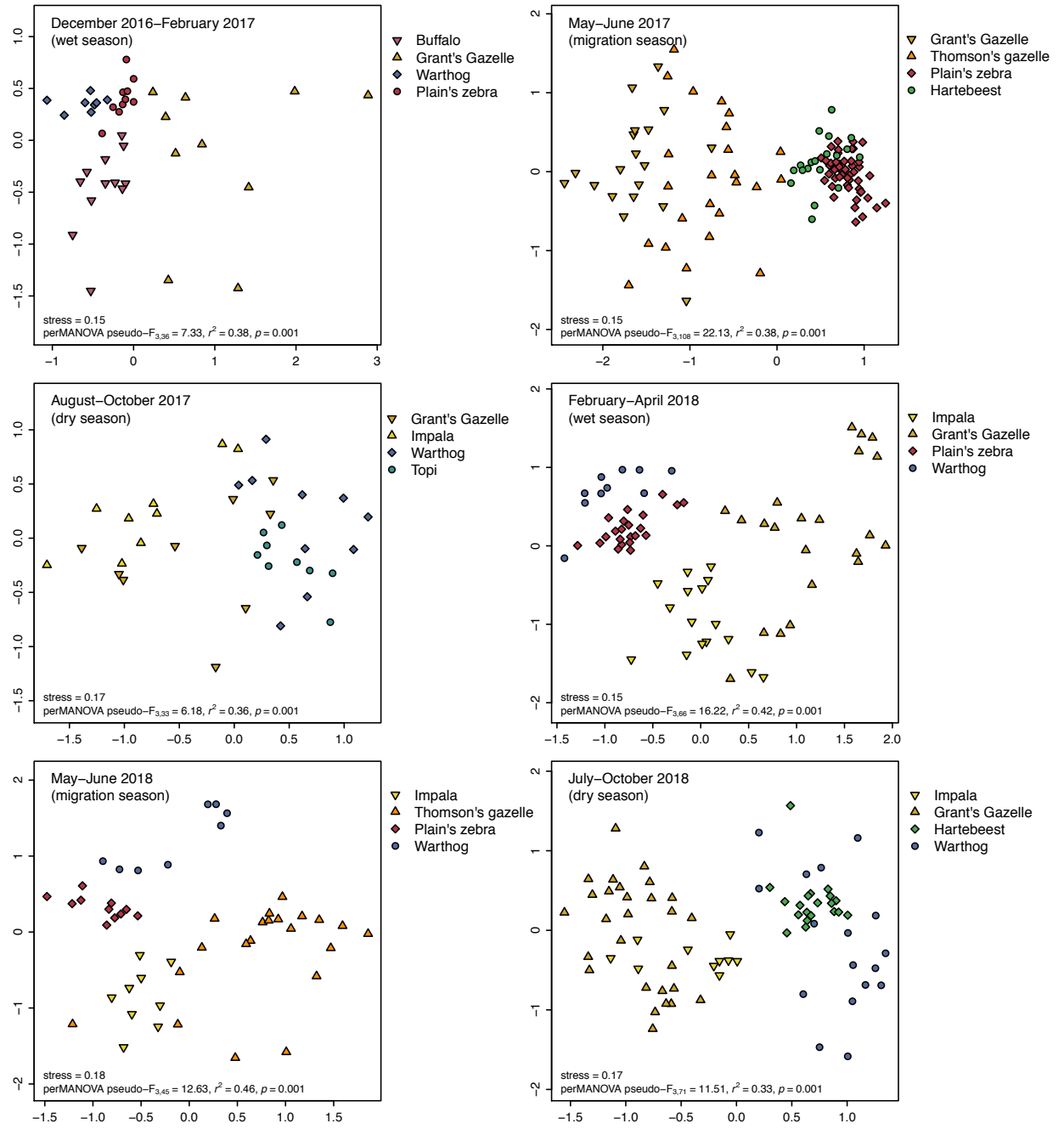

S7C. Gorongosa National Park, Mozambique. All species represented by $n \geq 10$ samples per bout. Data from 2017 (top right, bottom left) do not exhibit clear grazer-browser separation because impala was the only sampled species with a predominantly browse-based diet.

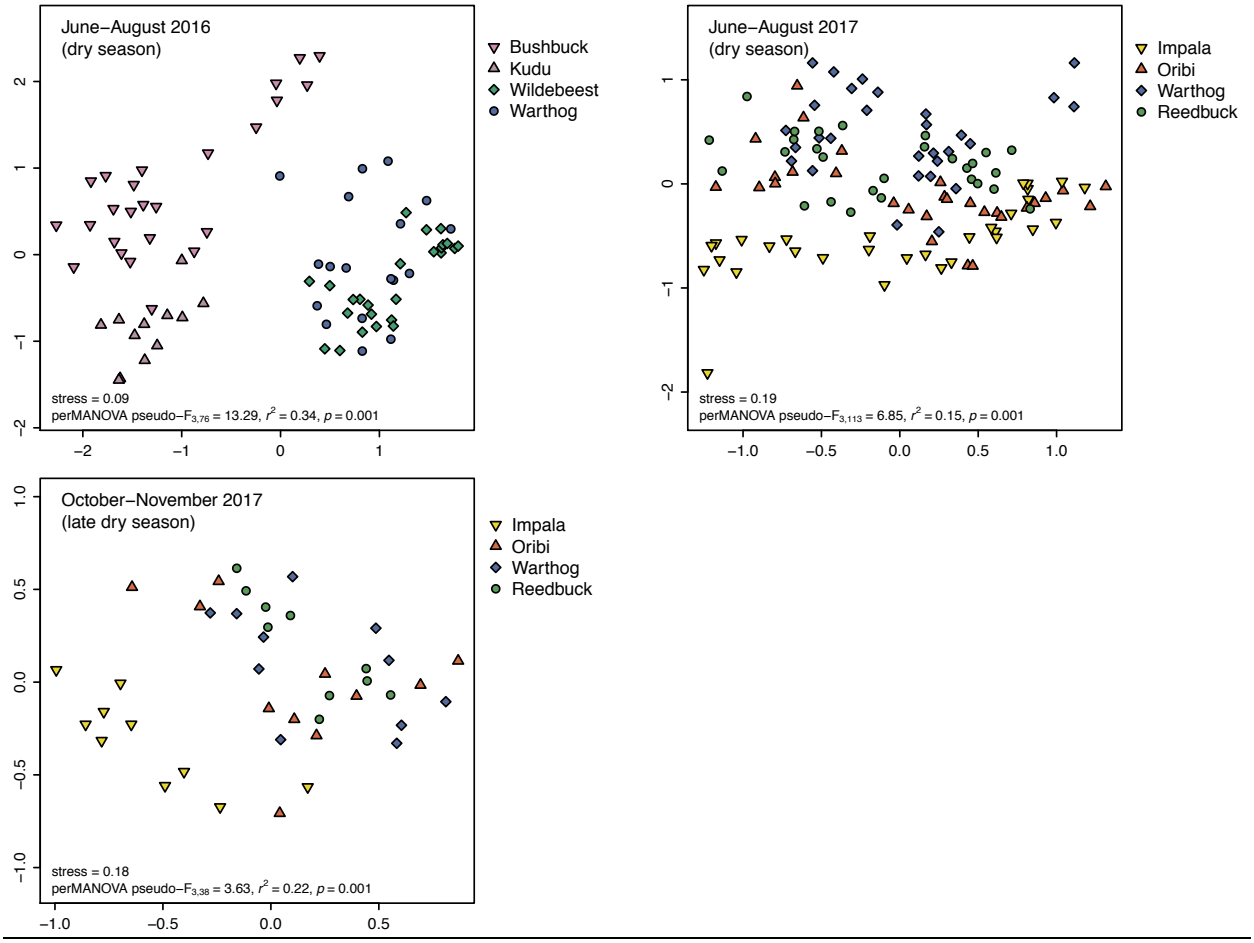

S7D. Addo Elephant National Park, South Africa. All species represented by $n \geq 10$ samples per bout. For a more visually discernible presentation of dietary dissimilarity between the browsers kudu and bushbuck in July 2013–February 2014, see **Fig. S8E**.

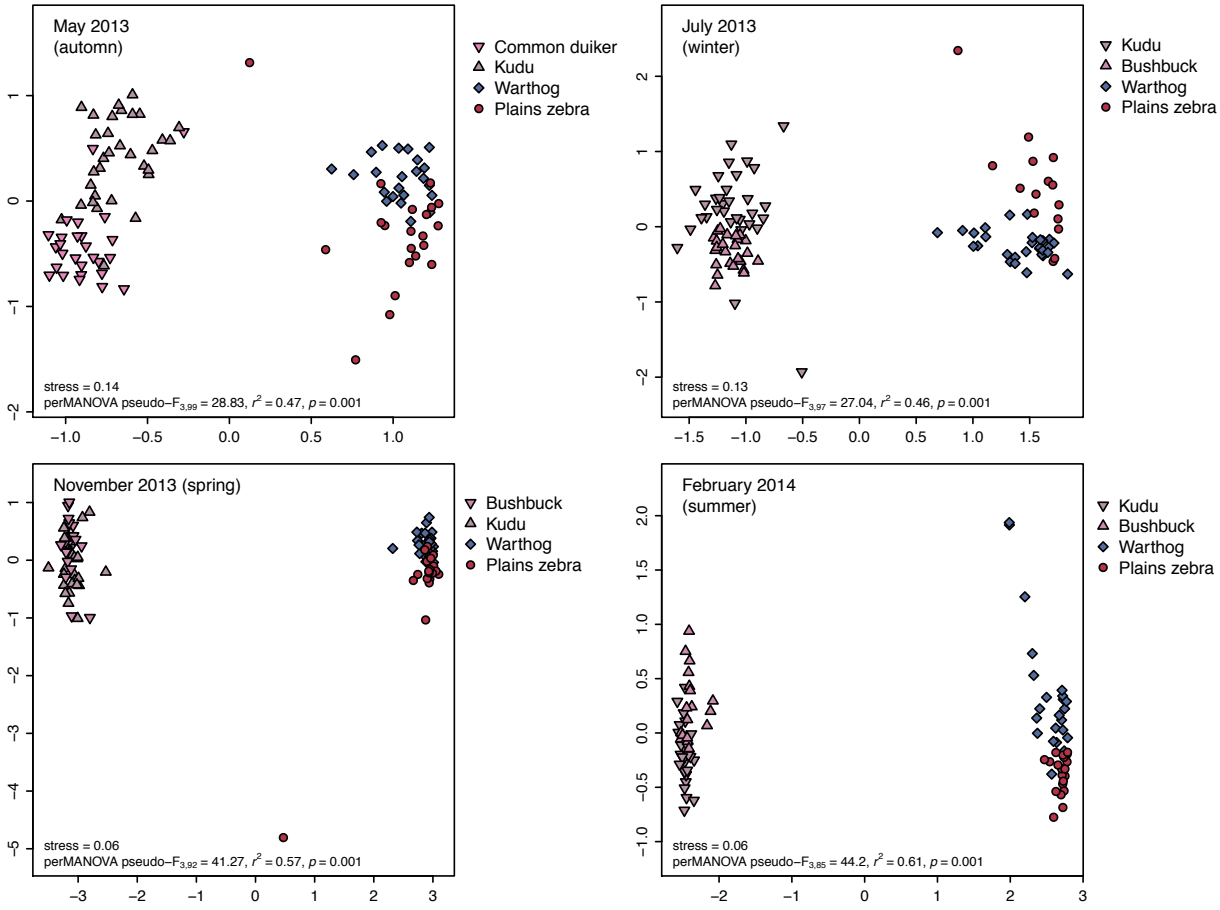

Figure S8. Ordinations of dietary dissimilarity among sets of closely related sympatric species. **(A)** Plains and Grevy's zebras (*Equus* spp.) in Laikipia; **(B)** hartebeest, wildebeest, and topi (tribe Alcelaphini) in Serengeti; **(C)** Grant's and Thomson's gazelles (tribe Antilopini) in Serengeti; **(D)** warthog and bushpig (subfamily Suinae) in Addo; **(E)** spiral-horned antelopes (*Tragelaphus* spp.) in Addo. **(F)** Comparisons from assorted sites: *Tragelaphus* spp. in Laikipia, Nyika, and Gorongosa, and waterbuck and puku (*Kobus* spp.) in Kafue. Stress value and permutational analysis of variance (perMANOVA) testing for significant differences among species are shown in each graph; ellipses show 1 SD. To maximize the number of possible comparisons in this supplementary analysis, we relaxed the sample-size threshold used for our main analyses (n = 10 per bout) to n = 8 (species included by virtue of relaxing the sample-size threshold are listed in the heading of each panel).

S8A. Plains and Grevy's zebras (*Equus* spp.) in Laikipia, Kenya. Sample-size threshold was relaxed for Grevy's zebra in 2016 (n = 9).

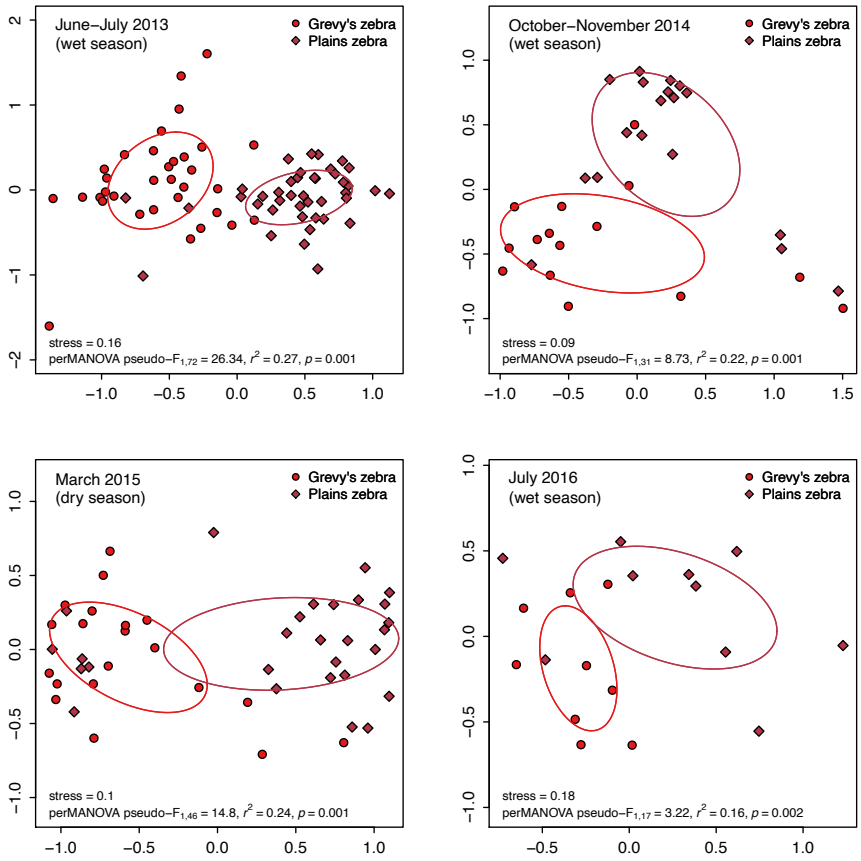

S8B. Tribe Alcelaphini in Serengeti National Park, Tanzania. Hartebeest, topi, and wildebeest in May–June 2017 (upper left), August–October 2017 (upper right), and February–March 2018 (center left); topi and wildebeest in May–June 2018 (center right); hartebeest and topi in July–October 2018 (bottom). Sample-size threshold was relaxed for topi in August–October 2017 (n = 9) and May–June 2018 (n = 8).

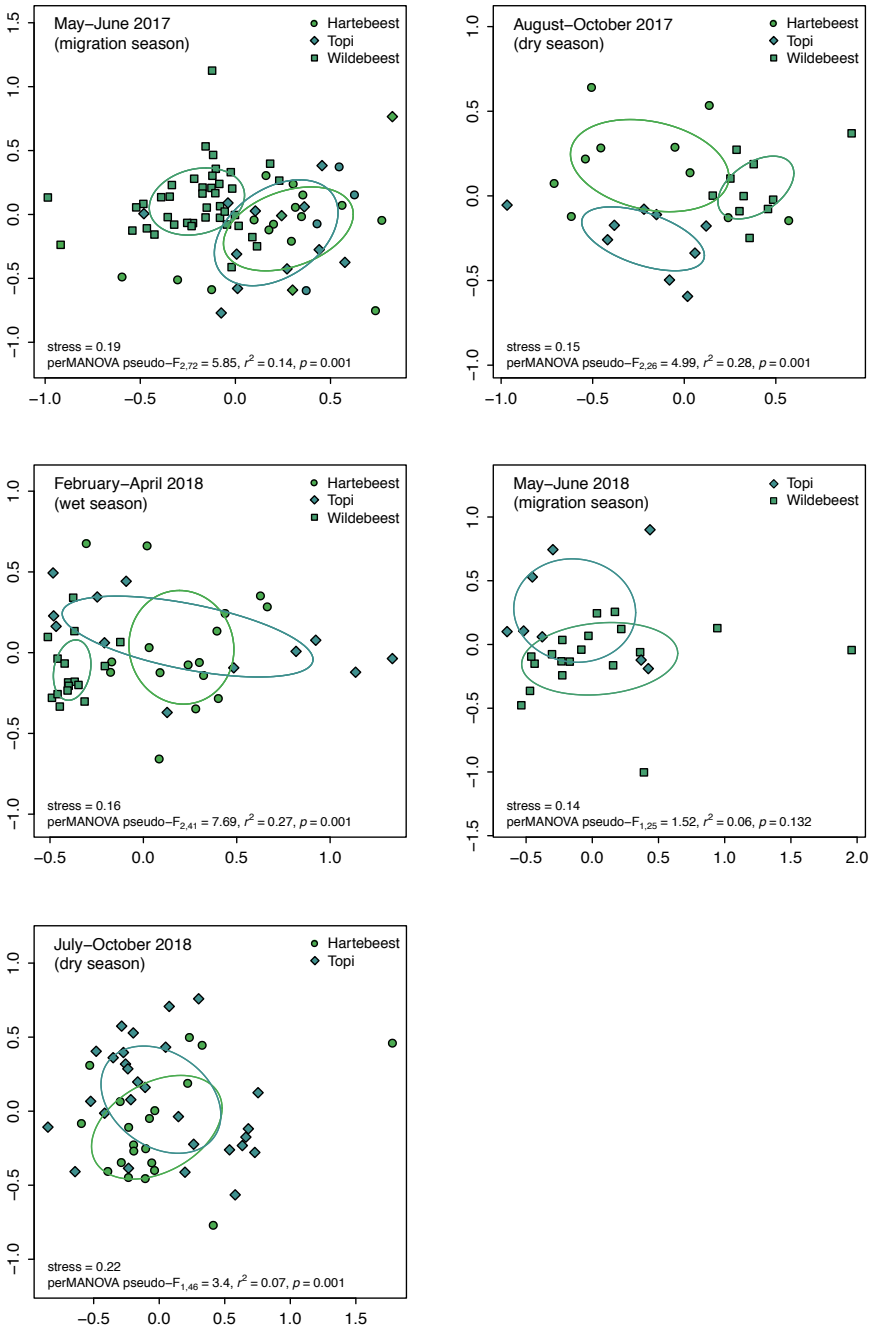

S8C. Grant's and Thomson's gazelles (tribe Antilopini) in Serengeti National Park, Tanzania. Sample-size threshold was relaxed for Grant's gazelle in August–October 2017 (n = 9).

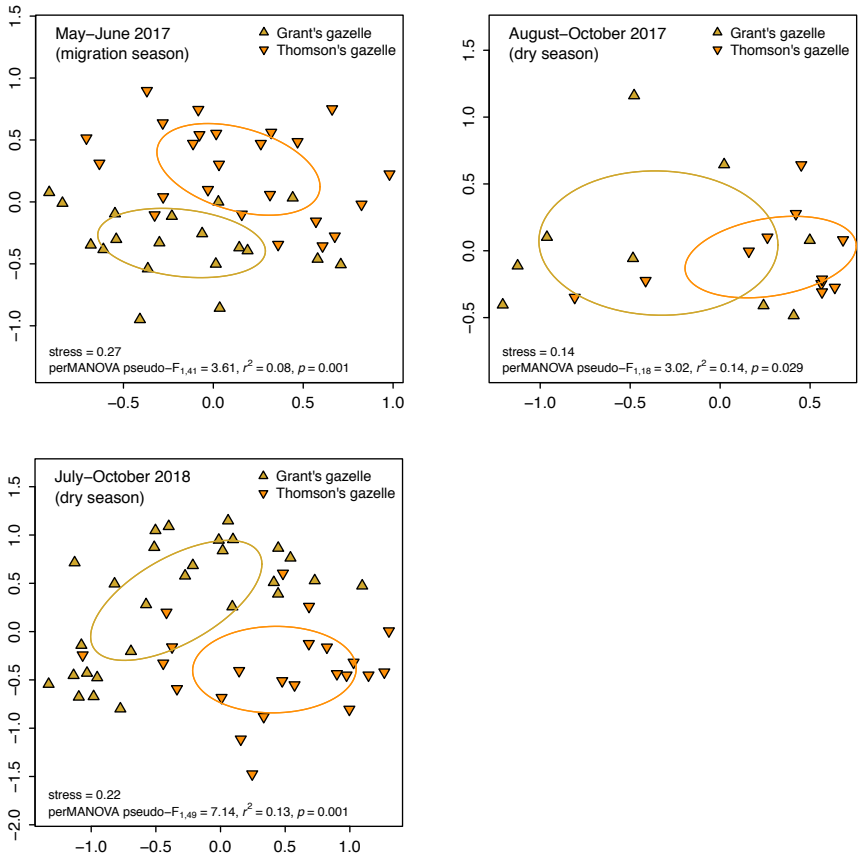

S8D. Bushpig and warthog (subfamily Suinae) in Addo Elephant National Park, South Africa. All species represented by $n \geq 10$ samples per bout.

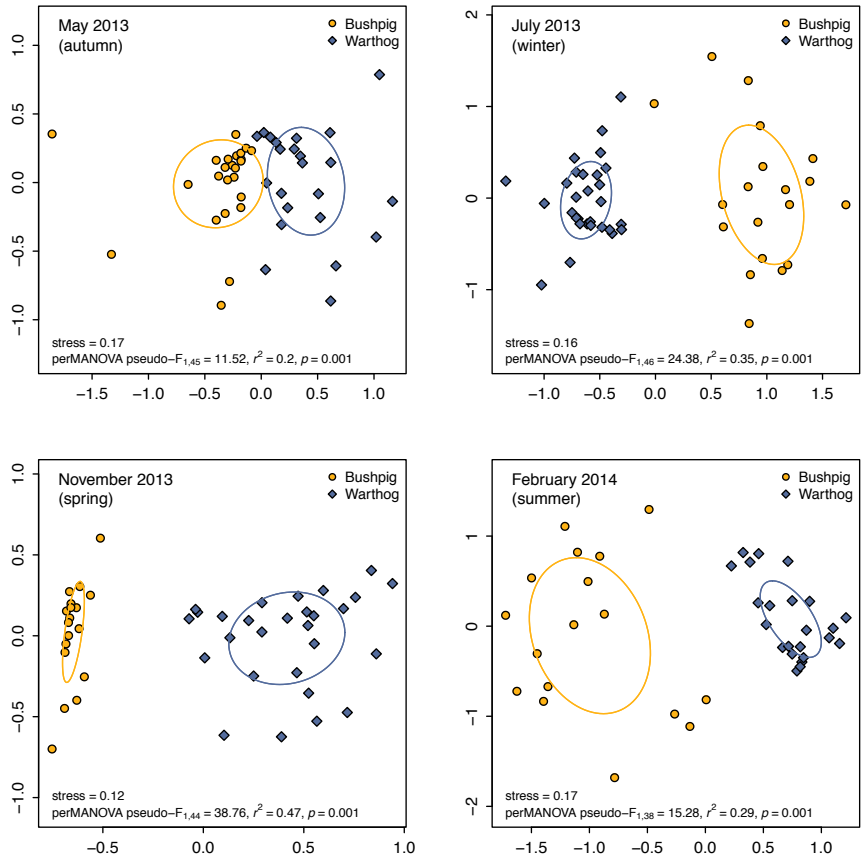

S8E. Bushbuck, eland, and kudu (*Tragelaphus* spp.) in Addo Elephant National Park, South Africa. All species represented by $n \geq 10$ samples per bout.

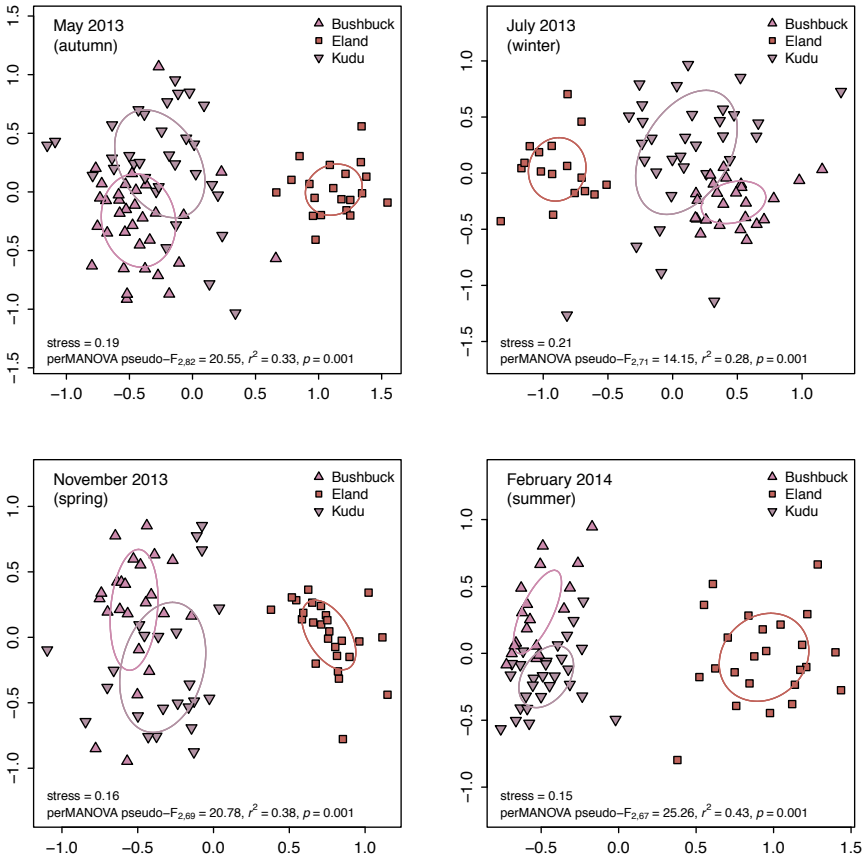

S8F. Additional comparisons from assorted sites. Eland and kudu (*Tragelaphus* spp.) in Laikipia in October–November 2014 (upper left); bushbuck and eland (*Tragelaphus* spp.) in Nyika National Park, Malawi, in August 2017 (upper right); bushbuck, kudu and nyala (*Tragelaphus* spp.) in Gorongosa National Park, Mozambique, in June–August 2016 (bottom left); and waterbuck and puku (*Kobus* spp.) in Kafue National Park, Zambia, in August 2017 (bottom right). Sample-size threshold was relaxed for kudu in Laikipia (n = 8) and waterbuck in Kafue (n = 9).

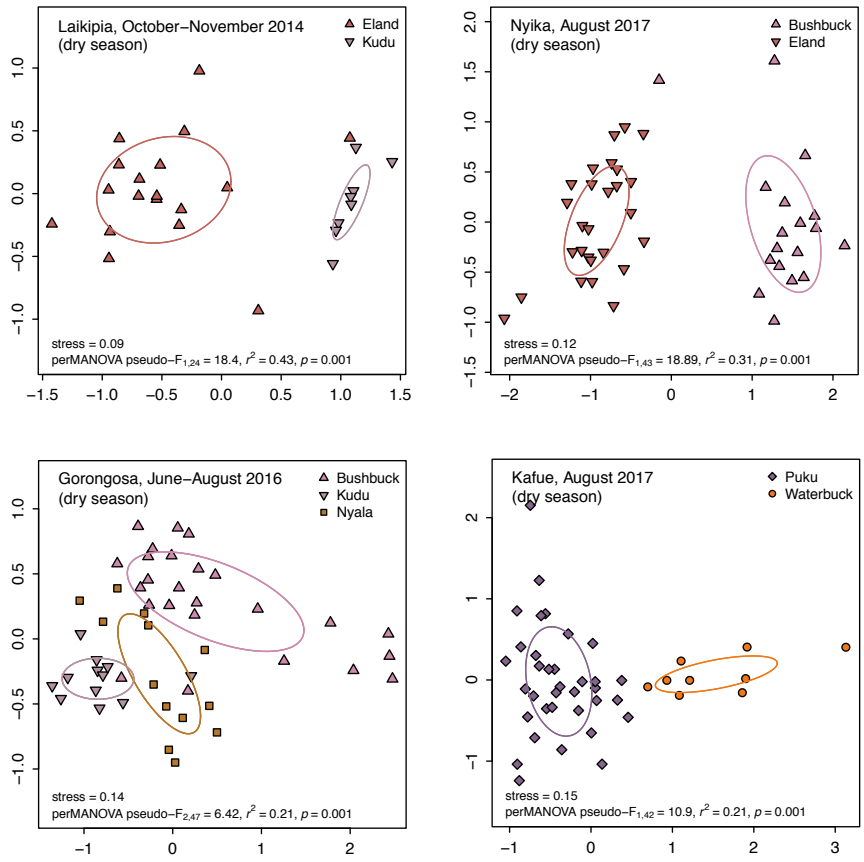

Figure S9. Within-species vs. between-species dietary dissimilarity at each site. Each pair of colored bars shows the distribution of Bray-Curtis dissimilarity values in comparisons between each pair of fecal samples from different species (green) and from the same species (orange) at each site. Bray-Curtis distance was calculated only between samples collected during the same sampling bout at each site, but all contrasts per site are shown together for clarity. Boxes show interquartile range, centerlines show median, whiskers extend up to 1.5 × IQR, points are outliers. Asterisks indicate that dietary dissimilarity was always significantly greater between than within species (*t*-test, all $p < 0.0001$). Note however that the discrepancy was weakest in Gorongosa, reflecting both a large number of interspecific comparisons with low dissimilarity (long tail of points) and anomalously high intraspecific dissimilarity (reflecting high individual variation/dispersion in several abundant species; **Fig. S6**).

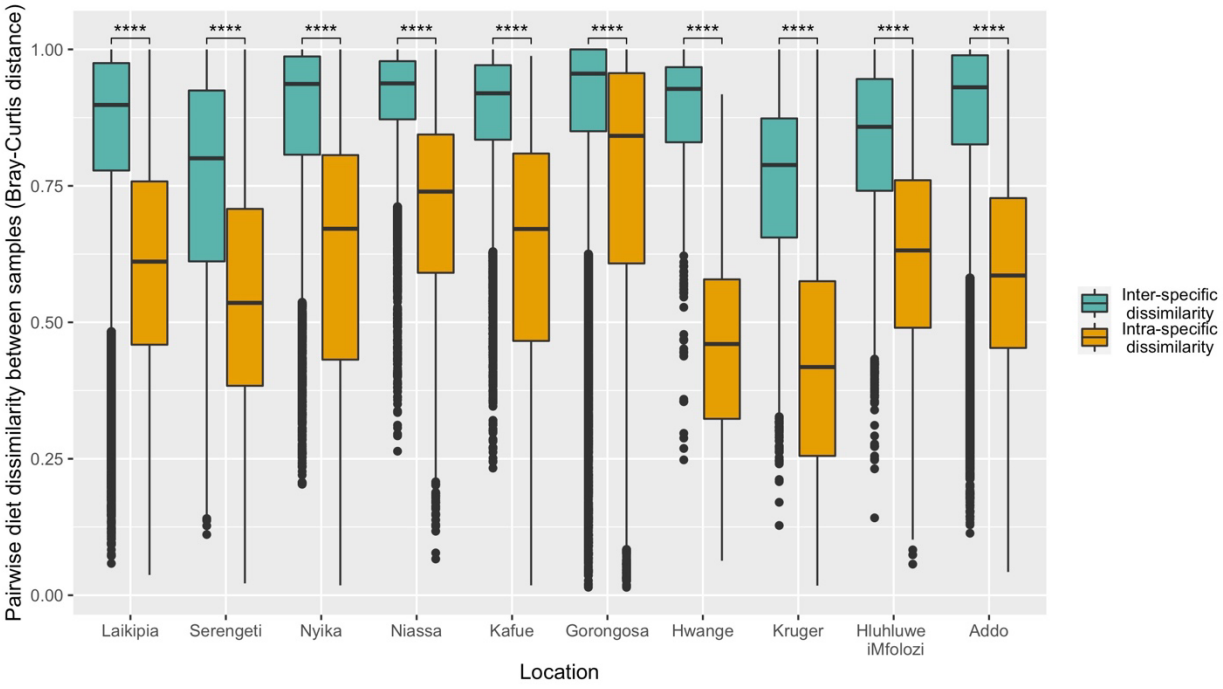

Figure S10. Frequency and strength of pairwise interspecific differences in diet composition. **(A)** Bars show the percentage of statistically significant pairwise contrasts of dietary dissimilarity between sympatric species within each site and sampling bout (perMANOVA, $p < 0.05$ after adjusting for multiple comparisons using the Holm method). The total number of pairwise comparisons per bout is shown above each bar. **(B)** Boxplots show the distribution of corresponding r^2 values from these pairwise perMANOVA for each site and bout, representing the proportion of variance in dietary dissimilarity explained by herbivore species identity; high r^2 values indicate low interspecific overlap, low values indicate high interspecific overlap. Boxes show interquartile range, centerlines show median, whiskers extend up to 1.5 × IQR, points are outliers. Dashed horizontal line shows median of all r^2 values. Full results for each pairwise perMANOVA (n = 723) are in **Dataset S25**.

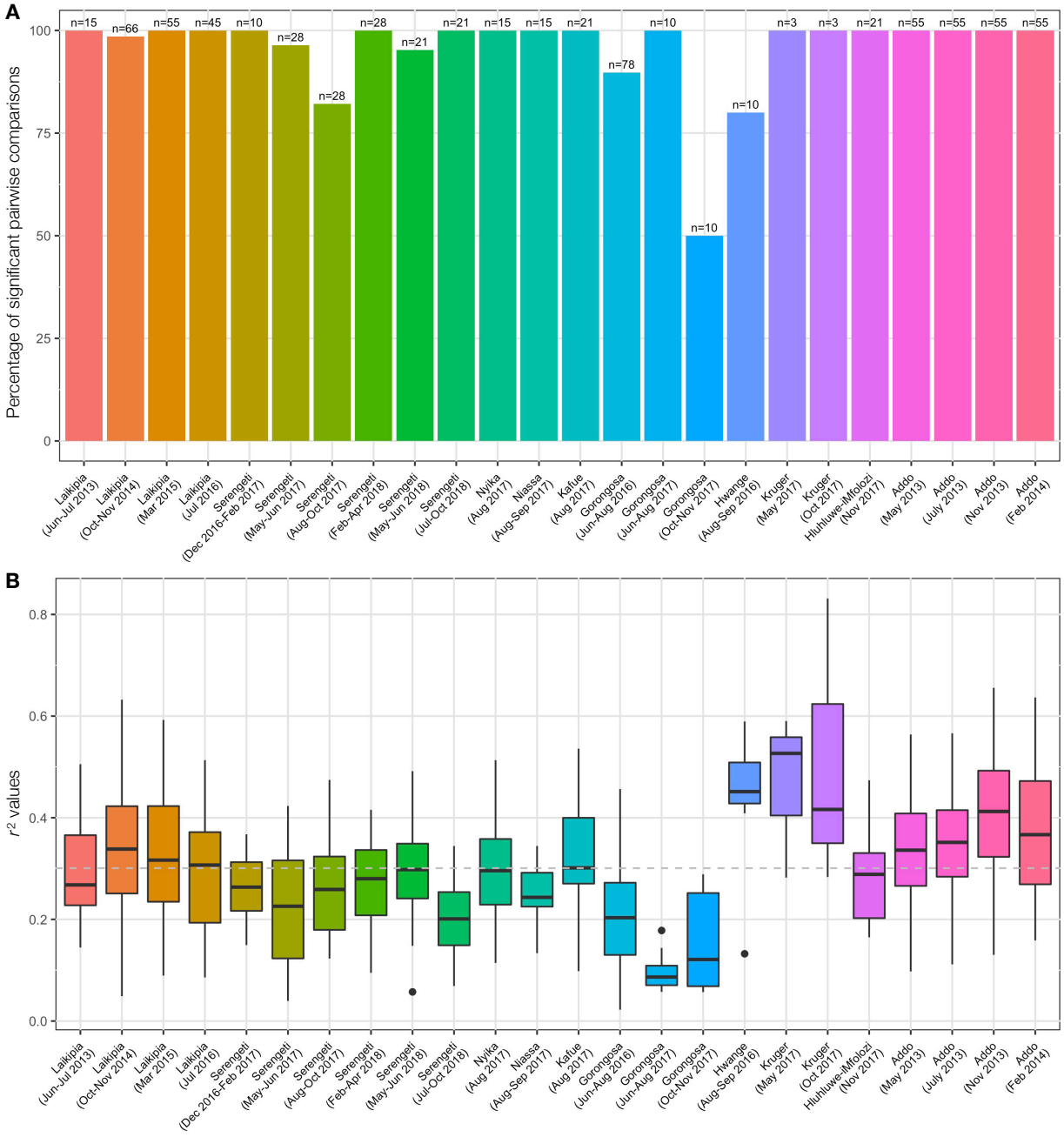

Figure S11. Correlates of the strength of pairwise interspecific differences in diet composition. One-way analyses of the r^2 values from pairwise perMANOVA of dietary dissimilarity between species in each site and bout (n = 723; **Fig. S10B**). Each panel corresponds to one of the fixed-effects in our candidate set of linear mixed-effects models (**Table S4**), where site was included as a random effect; our inferences are based on those models, but we show these one-way relationships to guide intuition. The strength of pairwise niche differences was **(A)** negatively correlated with rainfall in the 90 d prior to sample collection and **(B)** positively correlated with difference in body-size between species. **(C)** Differences in diet composition were strongest between pairs of nonruminants and weakest between pairs of ruminants. **(D)** The strength of pairwise dietary differentiation increased with the difference in proportional grass consumption between species, which is trivial (see **Text S2**), although note the considerable scatter in this relationship (i.e., sympatric species could have strong differences in diet composition even when they occupied the same position along the grazer-browser spectrum; **Fig. S7**).

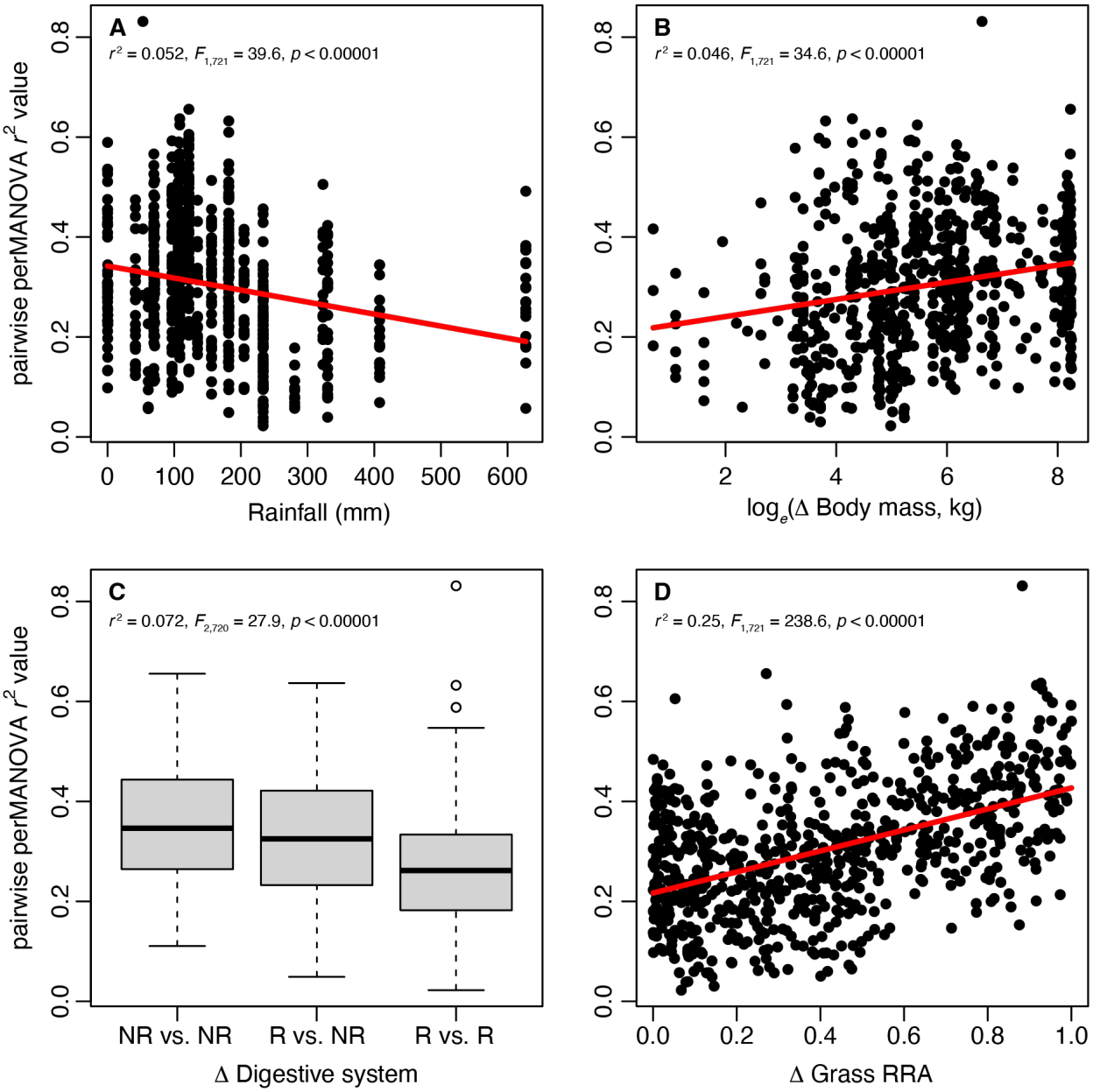

SUPPLEMENTARY TABLES

Table S1. Site characteristics. Salient attributes of the 10 sites sampled in this study. Major habitat types are World Wildlife Fund (WWF) categories (41); where more than one category overlapped a site, we list the one covering the majority of the area. Protected area locations and sizes were extracted from the World Database on Protected Areas (www.protectedplanet.net). We provide brief verbal descriptions of the habitat and dominant vegetation in each site. Mean annual temperature and precipitation (MAP) were extracted from WorldClim data (1961–1990), averaged across ~1 km^2 grid cells within each park (42). Dates of sampling bouts and rainfall 90 d prior to each are provided. The number of species sampled in each sampling bout is shown, along with the area of the minimum convex polygon (MCP) encompassing 95% of samples and any pertinent notes about each site.

Country	Location	WWF Major Habitat Type	Lat.	Long.	Area (km^2)	Area sampled	Avg. Temp. (°C)	MAP (mm)	Sampling bouts and rainfall 90-d prior sampling (mm)	No. species sampled	95% MCP (km^2)	Notes
Kenya (KEN)	Laikipia (Mpala and Ol Jogi Conservancies)	Tropical and Subtropical Grasslands, Savannas, & Shrublands (TSGSS)	0.37	36.93	461	Entire location, comprising semi-arid *Acacia* bushland and discontinuous understory of grasses, forbs, and subshrubs	18	695	(1) June-July 2013 (323 mm) (2) Oct.-Nov. 2014 (182 mm) (3) Mar. 2015 (97 mm) (4) July 2016 (156 mm)	(1) 6 (2) 12 (3) 11 (4) 13	(1) 106 (2) 68 (3) 90 (4) 151	Private conservancies managed for wildlife and low-density livestock (mostly cattle). Fauna largely historically intact, but rhino present only on Ol Jogi.
Tanzania (TAN)	Serengeti National Park	TSGSS	-2.34	34.78	13039	Central part (Snapshot Serengeti grid), comprising open grassland, woodland savanna, and kopjes	21	946	(1) Dec. 2016-Feb. 2017 (181 mm) (2) May-June 2017 (330 mm) (3) Aug.-Oct. 2017 (42 mm) (4) Feb.-Apr. 2018 (205 mm) (5) May-June 2018 (627 mm) (6) July-Oct. 2018 (408 mm)	(1) 5 (2) 8 (3) 8 (4) 8 (5) 7 (6) 7	(1) 457 (2) 499 (3) 267 (4) 835 (5) 619 (6) 670	Assemblage dominated by grazers and marked by annual great migration of wildebeest, zebra, and Thomson's gazelle
Malawi (MAW)	Nyika National Park	Montane Grasslands & Shrublands (MGS)	-10.57	33.85	3092	Nyika plateau, comprising Afromontane grassland with patches of Afromontane forest	17	1220	August 2017 (71 mm)	6	352	Highest elevation (≥ 2000 m) among our sampling locations
Mozambique (MOZ)	Niassa National Reserve	TSGSS	-12.01	37.35	38198	Southeastern part (L5 South), comprising deciduous miombo savanna woodland	25	1178	August 2017 (0 mm)	6	149	Sampled during a very dry period (0 mm rainfall in 90 d prior to sampling)
Zambia (ZAM)	Kafue National Park	TSGSS	-15.16	25.87	22309	Northeastern part, comprising miombo woodland, shrubland, and grassland dambos	21	907	August 2017 (0 mm)	7	61	Sampled during a very dry period (0 mm rainfall in 90 d prior to sampling)
Mozambique (MOZ)	Gorongosa National Park	TSGSS	-18.82	34.50	3693	Southern part (south of Lake Urema), comprising floodplain grassland, *Acacia-Combretum*-palm savannas, sand forest, and termitaria thicket	25	1091	(1) June-Aug. 2016 (233 mm) (2) June-Aug. 2017 (281 mm) (3) Oct.-Nov. 2017 (61 mm)	(1) 13 (2) 5 (3) 5	(1) 350 (2) 59 (3) 49	Unique among locations in terms of intensity of human disturbance. All large-herbivore populations increasing following severe defaunation during Mozambican Civil War, but mid-sized ungulates dominant and predation low (leopard, wild dog, hyena absent)
Zimbabwe (ZIM)	Hwange National Park	TSGSS	-19.08	26.56	14651	Eastern part (Main camp area), comprising savanna bushland and deciduous woodland	21	547	August 2016 (0 mm)	5	~570	Limited coverage of herbivore assemblage (5 spp.) and limited sample sizes for all species except plains zebra (Fig. 2G). Sampled during a very dry period (0 mm rainfall in 90 d prior to sampling)
South Africa (RSA)	Kruger National Park	TSGSS	-24.02	31.49	19169	Central part (Satara area), comprising open savanna grassland (*Acacia* spp., *Sderocarya birrea*, *Dichrostadys cinerea*) on basalt	22	561	(1) May 2017 (107 mm) (2) October 2017 (53 mm)	(1) 3 (2) 3	(1) 20 (2) 9	Limited coverage of herbivore assemblage (6 spp.) and limited sample sizes for species sampled in October 2017 (giraffe, kudu, waterbuck; Fig. S2D)
South Africa (RSA)	Hluhluwe-iMfolozi Park	MGS	-28.26	31.90	897	Central and Northern parts, comprising grassland, savanna, thicket, and forest	21	894	November 2017 (135 mm)	7	370	High prevalence of megaherbivores in the large-herbivore assemblage, notably white rhino
South Africa (RSA)	Addo Elephant National Park	Mediterranean Forests, Woodlands, and Scrub	-33.39	25.60	1377	Southern part (Main Camp and Colchester areas), comprising Albany subtropical thicket	18	399	(1) May 2013 (106 mm) (2) July 2013 (69 mm) (3) November 2013 (122 mm) (4) February 2014 (108 mm)	(1) 11 (2) 11 (3) 11 (4) 11	(1) 38 (2) 49 (3) 38 (4) 22	Same set of herbivore species sampled consistently across seasons, but methodological differences in sample collection and analysis precluded use in direct comparative analyses

Table S2. Model-selection analysis for population-level dietary richness. Dietary richness was measured as the number of mOTUs in the diet of each population after rarefying to a common depth of n = 10 samples. Sample size was n = 119 population-bouts from 7 sites; populations sampled repeatedly at the same site were included separately, and all models included site as a random intercept. The null model included only an intercept and the random effect (**Text S2**). For each model, we report the numerator degrees of freedom (df), log-likelihood (logLik), Akaike information criterion (AIC_c), difference in AIC_c relative to the top model (ΔAIC_c), Akaike weight (w_i, the likelihood of a model's being the best in the set), marginal r^2 (proportion of variance explained by the fixed effects alone), conditional r^2 (proportion of variance explained by both fixed and random effects), fixed parameter estimates (± SE) and their statistical significance levels (* $p < 0.05$, ** $p < 0.01$, *** $p < 0.001$) along with the random effect variance (± SD). The 2 models with $\Delta AICc < 2$, indicating substantial empirical support, are in boldface. The relative variable importance for each fixed effect (RVI), obtained by summing w_i across all models containing that effect, is shown in the column heading for each term.

Rank	Model	df	logLik	AIC_c	ΔAIC_c	w_i	$r^2_{marginal}$	$r^2_{conditional}$	Fixed effect estimates ± SE						Random effect (site) variance ± SD
									Intercept	Grass RRA + Grasss RRA^2 (RVI = 1.00)		Digestion (RVI = 0.31)	Body mass (RVI = 0.25)	Rainfall (RVI = 0.41)	
1	**Grass RRA + Grass RRA2**	**5**	**-405.5**	**821.46**	**0**	**0.35**	**0.26**	**0.37**	**32.88 ± 1.78**	**26.02 ± 7.54 *****	**-35.74 ± 7.44 *****				**8.37 ± 2.89**
2	**Grass RRA + Grass RRA2 + log(Body mass)**	**6**	**-404.9**	**822.51**	**1.05**	**0.21**	**0.28**	**0.36**	**30.56 ± 2.70**	**24.39 ± 7.64 *****	**-34.59 ± 7.48 *****		**0.50 ± 0.45**		**6.75 ± 2.60**
3	Grass RRA + Grass RRA2 + Digestive system	6	-405.4	823.51	2.04	0.13	0.27	0.37	33.52 ± 2.33	26.08 ± 7.55 ***	-36.34 7.60 ***	-0.73174			7.84 ± 2.80
4	Grass RRA + Grass RRA2 + Rainfall	6	-405.5	823.67	2.21	0.12	0.27	0.37	32.97 ± 1.93	26.09 ± 7.60 ***	-35.82 ± 7.50 ***			-7E-04 ± 5E-03	8.02 ± 2.83
5	Grass RRA + Grass RRA2 + log(Body mass) + Rainfall	7	-404.9	824.75	3.29	0.07	0.28	0.36	30.66 ± 2.83	24.47 ± 7.69 **	-34.68 ± 7.55 ***		0.50 ± 0.45	-8E-04 ± 5E-03	6.43 ± 2.54
6	Grass RRA + Grass RRA2 + Digestive system + log(Body mass)	7	-404.9	824.77	3.3	0.07	0.28	0.36	30.55 ± 3.74	24.39 ± 7.69 **	-34.58 ± 7.77 ***	0.005 ± 1.89	0.50 ± 0.49		6.75 ± 2.60
7	Grass RRA + Grass RRA2 + Digestive system + Rainfall	7	-405.4	825.75	4.29	0.04	0.27	0.36	33.62 ± 2.43	26.16 ± 7.60 ***	-36.44 ± 7.65 ***	-0.74 ± 1.74		-8E-04 ± 5E-03	7.50 ± 2.74
8	Grass RRA + Grass RRA2 + Digestive system + log(Body mass) + Rainfall	8	-404.9	827.05	5.59	0.02	0.28	0.36	30.65 ± 3.82	24.47 ± 7.75 **	-34.68 ± 7.82 ***	0.005 ± 1.89	0.50 ± 0.49	-8E-04 ± 6E-03	6.43 ± 2.54
9	Digestive system +log(Body mass)	5	-420	850.47	29	0	0.07	0.22	24.08 ± 3.87			5.76 ± 1.78 **	0.99 ± 0.54		12.31 ± 3.51
10	Digestive system	4	-421.6	851.53	30.07	0	0.05	0.23	30.26 ± 2.05			4.45 ± 1.64 **			14.92 ± 3.86
11	Digestive system + log(Body mass) + Rainfall	6	-419.8	852.44	30.97	0	0.07	0.26	23.77 ± 4.03			5.73 ± 1.77 **	0.97 ± 0.54	4E-04 ± 7E-03	15.73 ± 4.00
12	Digestive system + Rainfall	5	-421.4	853.37	31.91	0	0.06	0.27	29.74 ± 2.37			4.45 ± 1.63 **		4E-04 ± 7E-03	18.99 ± 4.36
13	Null model	3	-425.1	856.46	35	0	0	0.15	33.16 ± 1.62						12.21 ± 3.49
14	log(Body mass)	4	-425	858.32	36.85	0	0	0.14	31.64 ± 3.14				0.28 ± 0.52		11.30 ± 3.36
15	Rainfall	4	-425	858.33	36.87	0	0	0.19	32.69 ± 2.03					4E-04 ± 7E-03	15.86 ± 3.98
16	log(Body mass) + Rainfall	5	-424.9	860.25	38.79	0	0	0.18	31.28 ± 3.38				0.27 ± 0.51	4E-04 ± 7E-03	14.79 ± 3.84

Table S3. Model-selection analysis for population-level dietary diversity. Dietary diversity was measured as the Shannon index for each population after rarefying to a common depth of $n = 10$ samples. Modelling approach, column headings, sample sizes, and statistical significance thresholds are as in **Table S2**. Here, random effect were very close to 0 in all models, suggesting that the inclusion of random intercepts may not have been necessary. However, we did not observe any major changes in the sign or significance of parameter estimates among the different models tested, suggesting that overfitting is not a concern; moreover, a model-selection analysis of dietary diversity using linear models without random effects produced identical results.

Rank	Model	df	logLik	AIC_c	ΔAIC_c	w_i	$r^2_{marginal}$	$r^2_{conditional}$	Fixed effect estimates ± SE						Random effect (site) variance ± SD
									Intercept	Grass RRA + Grasss RRA^2 (RVI = 1.00)		Digestion (RVI = 0.31)	Body mass (RVI = 0.25)	Rainfall (RVI = 0.41)	
1	**Grass RRA + Grass RRA^2**	**5**	**-36.62**	**83.76**	**0**	**0.29**	**0.16**	**0.16**	**2.34 ± 0.06**	**1.30 ± 0.34 *****	**-1.47 ± 0.34 *****				**3.7E-04 ± 0.02**
2	**Grass RRA + Grass RRA^2 + Rainfall**	**6**	**-35.79**	**84.34**	**0.57**	**0.22**	**0.17**	**0.17**	**2.30 ± 0.07**	**1.24 ± 0.34 *****	**-1.43 ± 0.34 *****			**3E-04 ± 2E-04**	**0.00 ± 0.00**
3	**Grass RRA + Grass RRA^2 + Digestive system**	**6**	**-36.21**	**85.17**	**1.41**	**0.14**	**0.16**	**0.16**	**2.29 ± 0.09**	**1.27 ± 0.34 *****	**-1.40 ± 0.35 *****	**0.07 ± 0.08**			**0.00 ± 0.00**
4	Grass RRA + Grass RRA^2 + log(Body mass)	6	-36.53	85.81	2.05	0.11	0.16	0.16	2.38 ± 0.11	1.32 ± 0.34 ***	-1.48 ± 0.34 ***		-0.008 ± 0.02		9.8E-05 ± 0.07
5	Grass RRA + Grass RRA^2 + Digestive system + Rainfall	7	-35.57	86.14	2.38	0.09	0.17	0.17	2.26 ± 0.09	1.23 ± 0.34 ***	-1.38 ± 0.34 ***	0.05 ± 0.08		3E-04 ± 2E-04	0.00 ± 0.00
6	Grass RRA + Grass RRA^2 + log(Body mass) + Rainfall	7	-35.76	86.54	2.77	0.07	0.17	0.17	2.33 ± 0.12	1.26 ± 0.34 ***	-1.44 ± 0.34 ***		-0.005 ± 0.02	3E-04 ± 2E-04	0.00 ± 0.00
7	Grass RRA + Grass RRA^2 + Digestive system + log(Body mass)	7	-36.21	87.43	3.67	0.05	0.16	0.16	2.29 ± 0.17	1.27 ± 0.35 ***	-1.40 ± 0.35 ***	0.07 ± 0.08	-3E-04 ± 0.02		0.00 ± 0.00
8	Grass RRA + Grass RRA^2 + Digestive system + log(Body mass) + Rainfall	8	-35.56	88.44	4.67	0.03	0.17	0.17	2.25 ± 0.17	1.23 ± 0.35 ***	-1.38 ± 0.35 ***	0.05 ± 0.09	0.001 ± 0.02	3E-04 ± 2E-04	0.00 ± 0.00
9	Digestive system	4	-44.1	96.55	12.79	0.00	0.04	0.04	2.33 ± 0.06			0.16 ± 0.07 *			0.00 ± 0.00
10	Digestive system + Rainfall	5	-43.53	97.59	13.83	0.00	0.05	0.05	2.29 ± 0.07			0.15 ± 0.07 *		3E-04 ± 2E-04	0.00 ± 0.00
11	Digestive system + log(Body mass)	5	-43.76	98.05	14.28	0.00	0.05	0.05	2.21 ± 0.16			0.18 ± 0.08 *	0.02 ± 0.02		0.00 ± 0.00
12	Digestive system + log(Body mass) + Rainfall	6	-43.12	98.99	15.23	0.00	0.06	0.06	2.15 ± 0.16			0.18 ± 0.08 *	0.02 ± 0.02	3E-04 ± 2E-04	0.00 ± 0.00
13	Null model	3	-46.54	99.29	15.53	0.00	0.00	0.00	2.44 ± 0.03						0.00 ± 0.00
14	Rainfall	4	-45.71	99.77	16.01	0.00	0.01	0.01	2.38 ± 0.06					3E-04 ± 2E-04	0.00 ± 0.00
15	log(Body mass)	4	-46.52	101.38	17.62	0.00	0.00	0.00	2.46 ± 0.12				-0.005 ± 0.02		0.00 ± 0.00
16	log(Body mass) + Rainfall	5	-45.71	101.94	18.18	0.00	0.01	0.01	2.39 ± 0.13				-0.002 ± 0.02	3E-04 ± 2E-04	0.00 ± 0.00

Table S4. Model-selection analysis of the strength of pairwise niche differentiation. Strength of niche differentiation was indexed using the r^2 values of pairwise perMANOVA of diet dissimilarity between contemporaneously sampled sympatric species. Sample size was n = 723 pairwise contrasts from all 10 sites (**Text S2**); of these, 89 did not meet the preferred minimum threshold of $n \geq 10$ samples, but model results are qualitatively equivalent when restricting the analysis to the 634 contrasts with $n \geq 10$ for both species. Site was included as a random intercept in all models; the null model included only an intercept and the random effect. For each model, we report the numerator degrees of freedom (df), log-likelihood (logLik), Akaike information criterion (AIC_c), difference in AIC_c relative to the top model (ΔAIC_c), Akaike weight (w_i, the likelihood of a model's being the best in the set), marginal r^2 (proportion of variance explained by the fixed effects alone), conditional r^2 (proportion of variance explained by both fixed and random effects), fixed parameter estimates (± SE) and their statistical significance levels ((*) $p < 0.10$, * $p < 0.05$, ** $p < 0.01$, *** $p < 0.001$) along with the random effect variance (± SD). The 2 models with $\Delta AICc < 2$, indicating substantial empirical support, are in boldface. The relative variable importance for each fixed effect (RVI), obtained by summing w_i across all models containing that effect, is shown in the column heading for each term. Because digestive system was specified as a categorical variable with 3 levels, this term has two parameters (RvsNR, ruminant vs. nonruminant; RvsR, ruminant vs. ruminant).

Rank	Model	df	logLik	AIC_c	ΔAIC_c	w_i	$r^2_{marginal}$	$r^2_{conditional}$	Fixed effect estimates ± SE						Random effect (site) variance ± SD
									Intercept	Grass RRA (RVI = 1.00)	Digestive system RvsNR (RVI = 0.13)	Digestive system RvsR (RVI = 0.13)	ΔBody mass (RVI = 1.00)	Rainfall (RVI = 0.65)	
1	**ΔGrass RRA + log(ΔBody mass) + Rainfall**	**6**	**705.78**	**-1399.4**	**0**	**0.56**	**0.27**	**0.54**	**0.17 ± 0.03**	**0.22 ± 0.01 *****			**0.011 ± 0.002 *****	**-6.7E-05 ± 3.7E-05 (*)**	**0.0046 ± 0.07**
2	**ΔGrass RRA + log(ΔBody mass)**	**5**	**704.15**	**-1398.2**	**1.22**	**0.31**	**0.26**	**0.55**	**0.16 ± 0.03**	**0.22 ± 0.01 *****			**0.011 ± 0.002 *****		**0.0051 ± 0.07**
3	ΔGrass RRA + ΔDigestive system + log(ΔBody mass) + Rainfall	8	705.90	-1395.6	3.85	0.08	0.27	0.54	0.18 ± 0.03	0.22 ± 0.01 ***	-0.0024 ± 0.012	-0.0054 ± 0.013	0.011 ± 0.002 ***	-6.6E-05 ± 3.7E-05 (*)	0.0046 ± 0.07
4	ΔGrass RRA + ΔDigestive system + log(ΔBody mass)	7	704.30	-1394.4	4.99	0.05	0.26	0.55	0.17 ± 0.03	0.22 ± 0.01 ***	-0.0025 ± 0.011	-0.0059 ± 0.012	0.011 ± 0.002 ***		0.0051 ± 0.07
5	ΔGrass RRA + ΔDigestive system + Rainfall	7	695.39	-1376.6	22.82	0.00	0.25	0.53	0.25 ± 0.03	0.21 ± 0.01 ***	-0.011 ± 0.012	-0.022 ± 0.012 (*)		-5.5E-05 ± 3.7E-05	0.0049 ± 0.07
6	ΔGrass RRA + Rainfall	5	693.31	-1376.5	22.91	0.00	0.25	0.53	0.24 ± 0.02	0.22 ± 0.01 ***				-5.7E-05 ± 3.7E-05	0.0050 ± 0.07
7	ΔGrass RRA + ΔDigestive system	6	694.30	-1376.5	22.96	0.00	0.24	0.54	0.25 ± 0.03	0.21 ± 0.01 ***	-0.010 ± 0.012	-0.023 ± 0.012 (*)			0.0054 ± 0.07
8	ΔGrass RRA	4	692.18	-1376.3	23.14	0.00	0.24	0.54	0.23 ± 0.02	0.22 ± 0.01 ***					0.0055 ± 0.07
9	ΔDigestive system + log(ΔBody mass)	6	555.39	-1098.7	300.79	0.00	0.02	0.33	0.31 ± 0.03		-0.0013 ± 0.014	-0.035 ± 0.015 *	0.004 ± 0.003		0.0056 ± 0.07
10	ΔDigestive system	5	554.23	-1098.4	301.06	0.00	0.02	0.33	0.34 ± 0.03		-0.0046 ± 0.014	-0.041 ± 0.015 **			0.0056 ± 0.08
11	ΔDigestive system + log(ΔBody mass) + Rainfall	7	555.42	-1096.7	302.76	0.00	0.02	0.33	0.31 ± 0.03		-0.0013 ± 0.014	-0.035 ± 0.015 *	0.005 ± 0.003	-1.2E-05 ± 4.5E-05	0.0054 ± 0.07
12	ΔDigestive system + Rainfall	6	554.25	-1096.4	303.06	0.00	0.02	0.33	0.34 ± 0.03		-0.0046 ± 0.014	-0.042 ± 0.015 **		-8.3E-06 ± 4.5E-05	0.0056 ± 0.07
13	log(ΔBody mass)	4	548.54	-1089.0	310.42	0.00	0.01	0.32	0.27 ± 0.03				0.007 ± 0.003 **		0.0057 ± 0.08
14	log(ΔBody mass) + Rainfall	5	548.60	-1087.1	312.33	0.00	0.01	0.31	0.28 ± 0.03				0.007 ± 0.003 **	-1.6E-05 ± 4.5E-05	0.0055 ± 0.07
15	Null model	3	545.17	-1084.3	315.14	0.00	0.00	0.32	0.32 ± 0.03						0.0059 ± 0.08
16	Rainfall	4	545.19	-1082.3	317.12	0.00	0.00	0.32	0.32 ± 0.03					-1.0E-05 ± 4.6E-05	0.0058 ± 0.08

SUPPLEMENTARY DATASET LEGENDS

Datasets S1–S24. Mean population-level relative read abundance (RRA) of plant mOTUs. These datasets are provided in Microsoft Excel format, with one spreadsheet per sampling bout.

Dataset S1: Laikipia, Kenya (June-July 2013)
Dataset S2: Laikipia, Kenya (October-November 2014)
Dataset S3: Laikipia, Kenya (March 2015)
Dataset S4: Laikipia, Kenya (July 2016)
Dataset S5: Serengeti National Park, Tanzania (December 2016-February 2017)
Dataset S6: Serengeti National Park, Tanzania (May-June 2017)
Dataset S7: Serengeti National Park, Tanzania (August-October 2017)
Dataset S8: Serengeti National Park, Tanzania (February-April 2018)
Dataset S9: Serengeti National Park, Tanzania (May-June 2018)
Dataset S10: Serengeti National Park, Tanzania (July-October 2017)
Dataset S11: Nyika National Park, Malawi (August 2017)
Dataset S12: Niassa National Reserve, Mozambique (August 2017)
Dataset S13: Kafue National Park, Zambia (August 2017)
Dataset S14: Gorongosa National Park, Mozambique (June-August 2016)
Dataset S15: Gorongosa National Park, Mozambique (June-August 2017)
Dataset S16: Gorongosa National Park, Mozambique (October-November 2017)
Dataset S17: Hwange National Park, Zimbabwe (August-September 2016)
Dataset S18: Kruger National Park, South Africa (May 2017)
Dataset S19: Kruger National Park, South Africa (October 2017)
Dataset S20: Hluhluwe-iMfolozi Park, South Africa (November 2017)
Dataset S21: Addo Elephant Park, South Africa (May 2013)
Dataset S22: Addo Elephant Park, South Africa (July 2013)
Dataset S23: Addo Elephant Park, South Africa (November 2013)
Dataset S24: Addo Elephant Park, South Africa (February 2014)

Column headings:

1. ***Sequence ID*:** Unique sequence identifier
2. ***Order name*:** Order of the plant taxon according to the database that provided the best identity score
3. ***Family name*:** Family of the plant taxon according to the database that provided the best identity score
4. ***Genus name*:** Genus of the plant taxon according to the database that provided the best identity score
5. ***Species name*:** Species of the plant taxon according to the database that provided the best identity score
6. ***Scientific name*:** Binomial of the taxon according to the database that provided the best identity score
7. ***Taxid*:** European Molecular Biology Laboratory (EMBL) TaxID of the scientific name
8. ***Best reference database*:** Reference database that provided the best assignment (MRC: Laikipia, Kenya; SER: Serengeti National Park; PNG: Gorongosa National Park; GDB: Global reference database). This column is not included for data from Addo Elephant National Park, where sequences were assigned only to a local reference database (the Addo local reference database was not used for assignments at other sites).
9. ***Best identity score*:** Best identity score with the closest sequence in the database that provided the best identity score. This column is not included for Addo Elephant National Park where sequences with only a perfect match were retained (i.e., *Best identity score* = 1).
10. ***Sequence*:** DNA sequence
11. ***Mean RRA per population:*** Mean relative read abundance (RRA) of each mOTU in the diet of each population. The number of samples analyzed for each species in that sampling bout is shown parenthetically; note that these tables include summary data for populations that we do not analyze in the study because the sample size per bout was insufficient (i.e., $n < 10$, except where explicitly noted in the text and captions).

Dataset S25. PerMANOVA of dietary dissimilarity between 723 pairs of sympatric species. This dataset is provided in Microsoft Excel format.

Column headings:

1. ***Site_no:*** Sites are numbered from 1 (northernmost) to 10 (southernmost)
2. ***Site:*** Name of the sampling site where the comparison was made
3. ***Bout:*** Temporal period (Month-Year) for which the comparison was made
4. ***Code_bout:*** Merged identifier specifying site, year, and season
5. ***Rainfall_mm:*** Rainfall, in mm, in the 90 d preceding sampling at each site
6. ***Spp_pair:*** Common names of the two species in each pairwise comparison
7. **Δmass:** Difference in body mass (absolute value) between the two species
8. **Δ*grass:*** Difference in proportional grass consumption (absolute value) between the two species
9. **Δ*digs:*** Difference (or equivalence) of digestive system between the two species (R, ruminant; NR, nonruminant)
10. ***N_thresh:*** Indicates whether both species in the comparison were above the preferred minimum sampling depth threshold of $n \geq 10$ samples
11. ***F_model:*** *F*-statistic of the perMANOVA model
12. ***r2:*** Coefficient of determination for the perMANOVA model, which represents the proportion of variance in dietary dissimilarity explained by herbivore species identity (high r^2 values indicate low interspecific dietary overlap, low values indicate higher interspecific overlap)
13. ***p:*** Uncorrected *p* value of the perMANOVA
14. ***adj_p:*** Adjusted *p*-value corrected for multiple comparisons within sampling bouts using the Holm method

SI REFERENCES

1. S. Willows-Munro, T. J. Robinson, C. A. Matthee, Utility of nuclear DNA intron markers at lower taxonomic levels: Phylogenetic resolution among nine *Tragelaphus* spp. *Mol. Phylogenet. Evol.* **35**, 624–636 (2005).
2. K. E. Jones, *et al.*, PanTHERIA: A species-level database of life history, ecology, and geography of extant and recently extinct mammals. *Ecology* **90**, 2648–2648 (2009).
3. T. R. Kartzinel, J. C. Hsing, P. M. Musili, B. R. P. Brown, R. M. Pringle, Covariation of diet and gut microbiome in African megafauna. *Proc. Natl. Acad. Sci. U. S. A.* **116**, 23588–23593 (2019).
4. T. R. Kartzinel, *et al.*, DNA metabarcoding illuminates dietary niche partitioning by African large herbivores. *Proc. Natl. Acad. Sci. U. S. A.* **112**, 8019–8024 (2015).
5. J. Pansu, *et al.*, Trophic ecology of large herbivores in a reassembling African ecosystem. *J. Ecol.* **107**, 1355–1376 (2019).
6. P. Taberlet, *et al.*, Power and limitations of the chloroplast *trn*L (UAA) intron for plant DNA barcoding. *Nucleic Acids Res.* **35**, e14 (2007).
7. J. Binladen, *et al.*, The use of coded PCR primers enables high-throughput sequencing of multiple homolog amplification products by 454 parallel sequencing. *PLoS One* **2**, e197 (2007).
8. A. Valentini, *et al.*, New perspectives in diet analysis based on DNA barcoding and parallel pyrosequencing: The *trn*L approach. *Mol. Ecol. Resour.* **9**, 51–60 (2009).
9. G. F. Ficetola, *et al.*, Replication levels, false presences and the estimation of the presence/absence from eDNA metabarcoding data. *Mol. Ecol. Resour.* **15**, 543–556 (2015).
10. F. Boyer, *et al.*, obitools: A unix-inspired software package for DNA metabarcoding. *Mol. Ecol. Resour.* **16**, 176–182 (2016).
11. B. A. Gill, *et al.*, Plant DNA-barcode library and community phylogeny for a semi-arid East African savanna. *Mol. Ecol. Resour.* **19**, 838–846 (2019).
12. T. M. Anderson, J. Shaw, H. Olff, Ecology's cruel dilemma, phylogenetic trait evolution and the assembly of Serengeti plant communities. *J. Ecol.* **99**, 797–806 (2011).
13. G. F. Ficetola, *et al.*, An *In silico* approach for the evaluation of DNA barcodes. *BMC Genomics* **11**, 434 (2010).
14. R Core Team, R: a language and environment for statistical computing. *https://www.r-project.org* (2015).
15. E. Willerslev, *et al.*, Fifty thousand years of Arctic vegetation and megafaunal diet. *Nature* **506**, 47–51 (2014).
16. B. Gebremedhin, *et al.*, DNA metabarcoding reveals diet overlap between the endangered walia ibex and domestic goats - implications for conservation. *PLoS One* **11**, e0159133 (2016).
17. B. E. Deagle, *et al.*, Counting with DNA in metabarcoding studies: How should we convert sequence reads to dietary data? *Mol. Ecol.* **28**, 391–406 (2019).
18. B. L. Littleford-Colquhoun, *et al.*, The precautionary principle and dietary DNA metabarcoding: Commonly used abundance thresholds change ecological interpretation. *Mol. Ecol.* **31**, 1615–1626 (2022).
19. M. De Barba, *et al.*, DNA metabarcoding multiplexing and validation of data accuracy for diet assessment: Application to omnivorous diet. *Mol. Ecol. Resour.* **14**, 306–323 (2014).
20. P. Taberlet, *et al.*, Soil sampling and isolation of extracellular DNA from large amount of starting material suitable for metabarcoding studies. *Mol. Ecol.* **21**, 1816–1820 (2012).
21. G. I. H. Kerley, *et al.*, Diet shifts by adult flightless dung beetles *Circellium bacchus*, revealed using DNA metabarcoding, reflect complex life histories. *Oecologia* **188**, 107–115 (2018).
22. P. Taberlet, A. Bonin, L. Zinger, E. Coissac, *Environmental DNA for Biodiversity Research and*

Monitoring (Oxford University Press, 2018).
23. C. Giguet-Covex, *et al.*, Long livestock farming history and human landscape shaping revealed by lake sediment DNA. *Nat. Commun.* **5**, 3211 (2014).
24. D. I. Bolnick, *et al.*, The ecology of individuals: Incidence and implications of individual specialization. *Am. Nat.* **161**, 1–28 (2003).
25. T. R. Kartzinel, R. M. Pringle, Multiple dimensions of dietary diversity in large mammalian herbivores. *J. Anim. Ecol.* **89**, 1482–1496 (2020).
26. M. C. Hutchinson, A. P. Dobson, R. M. Pringle, Dietary abundance distributions: Dominance and diversity in vertebrate diets. *Ecol. Lett.* **25**, 992–1008 (2022).
27. D. R. Anderson, *Model Based Inference in the Life Sciences: A Primer on Evidence* (Springer, 2008).
28. J. Fox, S. Weisberg, *An R Companion to Applied Regression*, 3rd Ed. (Sage, 2019).
29. D. Bates, M. Mächler, B. M. Bolker, S. C. Walker, Fitting linear mixed-effects models using lme4. *J. Stat. Softw.* **67**, 1–48 (2015).
30. K. Barton, MuMIn: Multi-model inference. R package version 1.43.17. https://CRAN.R-project.org/package=MuMIn (2020).
31. W. J. Freeland, "Plant secondary metabolites: Biochemical coevolution with herbivores" in *Plant Defenses against Mammalian Herbivory*, R. T. Palo, C. T. Robbins, Eds. (CRC Press, 1991), pp. 61–81.
32. M. Clauss, P. Steuer, D. W. H. Müller, D. Codron, J. Hummel, Herbivory and body size: Allometries of diet quality and gastrointestinal physiology, and implications for herbivore ecology and dinosaur gigantism. *PLoS One* **8**, e68714 (2013).
33. A. W. Illius, I. J. Gordon, Modelling the nutritional ecology of ungulate herbivores: Evolution of body size and competitive interactions. *Oecologia* **89**, 428–434 (1992).
34. M. D. Dearing, K. D. Kohl, Beyond fermentation: Other important services provided to endothermic herbivores by their gut microbiota. *Integr. Comp. Biol.* **57**, 723–731 (2017).
35. A. C. Staver, G. P. Hempson, Seasonal dietary changes increase the abundances of savanna herbivore species. *Sci. Adv.* **6**, eabd2848 (2020).
36. R. M. Pringle, M. C. Hutchinson, Resolving food-web structure. *Annu. Rev. Ecol. Evol. Syst.* **51**, 55–80 (2020).
37. J. G. C. Hopcraft, H. Olff, A. R. E. Sinclair, Herbivores, resources and risks: Alternating regulation along primary environmental gradients in savannas. *Trends Ecol. Evol.* **25**, 119–128 (2010).
38. J. T. du Toit, H. Olff, Generalities in grazing and browsing ecology: Using across-guild comparisons to control contingencies. *Oecologia* **174**, 1075–1083 (2014).
39. A. B. Potter, *et al.*, Mechanisms of dietary resource partitioning in large-herbivore assemblages: A plant-trait-based approach. *J. Ecol.* **110**, 817–832 (2022).
40. D. Codron, C. B. Bousman, F. Buschke, M. Clauss, C. Lewis, Competition drives the evolution of emergent neutrality in the dietary niches of mammalian herbivores. *Quat. Int.* (2021) https:/doi.org/10.1016/j.quaint.2021.11.002.
41. D. M. Olson, *et al.*, Terrestrial ecoregions of the world: A new map of life on Earth. *Bioscience* **51**, 933–938 (2001).
42. R. J. Hijmans, S. E. Cameron, J. L. Parra, P. G. Jones, A. Jarvis, Very high resolution interpolated climate surfaces for global land areas. *Int. J. Climatol.* **25**, 1965–1978 (2005).